

JGR Solid Earth

RESEARCH ARTICLE

10.1029/2020JB021492

Key Points:

- At 85–80 Ma, the Mineoka ophiolite formed in the back-arc spreading of Nemuro–Olyutorsky arc, at paleolatitude of $N \sim 16^\circ$ in the NW Pacific
- The spreading was continued until 49 Ma and placed at paleolatitude of $N \sim 34^\circ$, following the Pacific Plate motion with a NE 60° orientation
- A small-sized, short-lived “Mineoka” plate existed shortly between the Philippine Sea Plate and the Pacific Plate, subducting below Japan

Supporting Information:

Supporting Information may be found in the online version of this article.

Correspondence to:

D. Pastor-Galán,
dpastorgalan@gmail.com







Citation:

Ganbat, A., Pastor-Galán, D., Hirano, N., Nakamura, N., Sumino, H., Yamaguchi, Y., & Tsujimori, T. (2021). Cretaceous to Miocene NW Pacific Plate kinematic constraints: Paleomagnetism and Ar–Ar geochronology in the Mineoka Ophiolite Mélange (Japan). *Journal of Geophysical Research: Solid Earth*, 126, e2020JB021492. <https://doi.org/10.1029/2020JB021492>

Received 7 DEC 2020

Accepted 27 APR 2021

Cretaceous to Miocene NW Pacific Plate Kinematic Constraints: Paleomagnetism and Ar–Ar Geochronology in the Mineoka Ophiolite Mélange (Japan)

Ariuntsetseg Ganbat¹ , Daniel Pastor-Galán^{1,2,3} , Naoto Hirano^{1,2} , Norihiro Nakamura¹ , Hirochika Sumino⁴ , Yuji Yamaguchi⁵, and Tatsuki Tsujimori^{1,2} 

¹Department of Earth Science, Graduate School of Science, Tohoku University, Sendai, Japan, ²Center for Northeast Asian Studies, Tohoku University, Sendai, Japan, ³Frontier Research Institute for Interdisciplinary Sciences, Tohoku University, Sendai, Japan, ⁴Graduate School of Arts and Sciences, University of Tokyo, Tokyo, Japan, ⁵Nippon Koei Limited, Tokyo, Japan

Abstract The Mineoka Ophiolite Mélange is located at the intersection of the Pacific, Philippine Sea, Eurasian, and North American plates. The Mineoka ophiolite origin is disputed, and it has been ascribed to a fully subducted plate or part of the Pacific and Philippine Sea plates. In this paper, we present a kinematic reconstruction of the Mineoka Ophiolite Mélange and its relation with the Pacific Plate, based on new paleomagnetic data and bulk-rock ⁴⁰Ar/³⁹Ar ages of basaltic rocks. In addition to standard analyses for paleolatitudes, we performed a Net tectonic rotation analysis on sheeted dolerite dikes to infer the paleospreading direction that formed the ophiolite. The analysis shows that 85–80 Ma MOR pillow basalts erupted at a paleolatitude of $N \sim 16^\circ$, whereas ~ 50 Ma basalts formed at $N \sim 34^\circ$. Net Tectonic Rotation analysis suggests that the spreading direction was NE 60° . Ar–Ar ages yielded 53–49 Ma for MORBs and 41–35 Ma for island-arc basalts. The formation of this ophiolite occurred in the back-arc spreading of the Nemuro–Olyutorsky arcs of the NW Pacific. It infers that the final consumption of Izanagi below Japan instigated a subduction jump and flipped its polarity. Subduction initiated parallel to the ridge, and a piece of the original back-arc crust got trapped near the Japan trench during the northwards motion of the Philippine Sea Plate. The contrasting motion between the Pacific and the Philippine Sea plates generated a highly unstable setting followed by a subduction zone that left a small-sized and short-lived plate (“Mineoka”), surrounded by subduction zones.

1. Introduction

East Asia has witnessed the birth and demise of oceanic plates at least, during the latest 500 million years. Subduction of numerous oceanic plates: Eurasian (Amur), Pacific, North America (Okhotsk), Indo-Australia, Caroline, and Philippine Sea plates formed a complex collage of ophiolites, volcanic arcs, orogenic belts, and continental fragments (i.e., terranes, blocks, and massifs) over East Asia (e.g., Hutchison, 1989; Isozaki et al., 2010; Maruyama & Seno, 1986; Metcalfe, 2011; Pastor-Galán et al., 2021; Seno & Maruyama, 1984; Wu et al., 2016). In addition to the onshore geological features, many different oceanic plates have been subducting since the Mesozoic until today, and left a mantle fingerprint that allows us to study and recognize several of these long-gone plates through mantle tomography (e.g., Li et al., 2008; Liu et al., 2020; Wu & Wu, 2019; Zahirovic et al., 2014). Altogether, East Asia represents one of the top places where we can investigate several of the long-standing problems of plate tectonics, including how plates reorganize, how a new super-oceanic plate develops, or how and when subduction initiates and terminates.

Ophiolites, fragments of the oceanic lithosphere on land, are the only providers of direct information about the subducted oceanic crust and are crucial to decipher the evolution of tectonic processes that occurred at seafloor spreading centers and subduction zones (e.g., Ishiwatari, 1994; Dilek, 2003; Furnes et al., 2020). The Mineoka Ophiolite Mélange (MOM) in the Boso Peninsula, Japan (Figure 1a) is an ophiolite mélange that tectonically emplaced in a unique tectonic setting where the Pacific, Philippine Sea Plate, Eurasia, and North American plates meet. This ophiolite mélange emplaced in the Japanese forearc together with the Cretaceous–Cenozoic Shimanto accretionary complex, by the Izu–Bonin collision zone, and also close to the trench–trench–trench type Boso triple junction in the NW Pacific (Hirano et al., 2003; Mori et al., 2011; Ogawa & Takahashi, 2004; Ogawa & Taniguchi, 1987; Takahashi et al., 2003). The ophiolite mélange

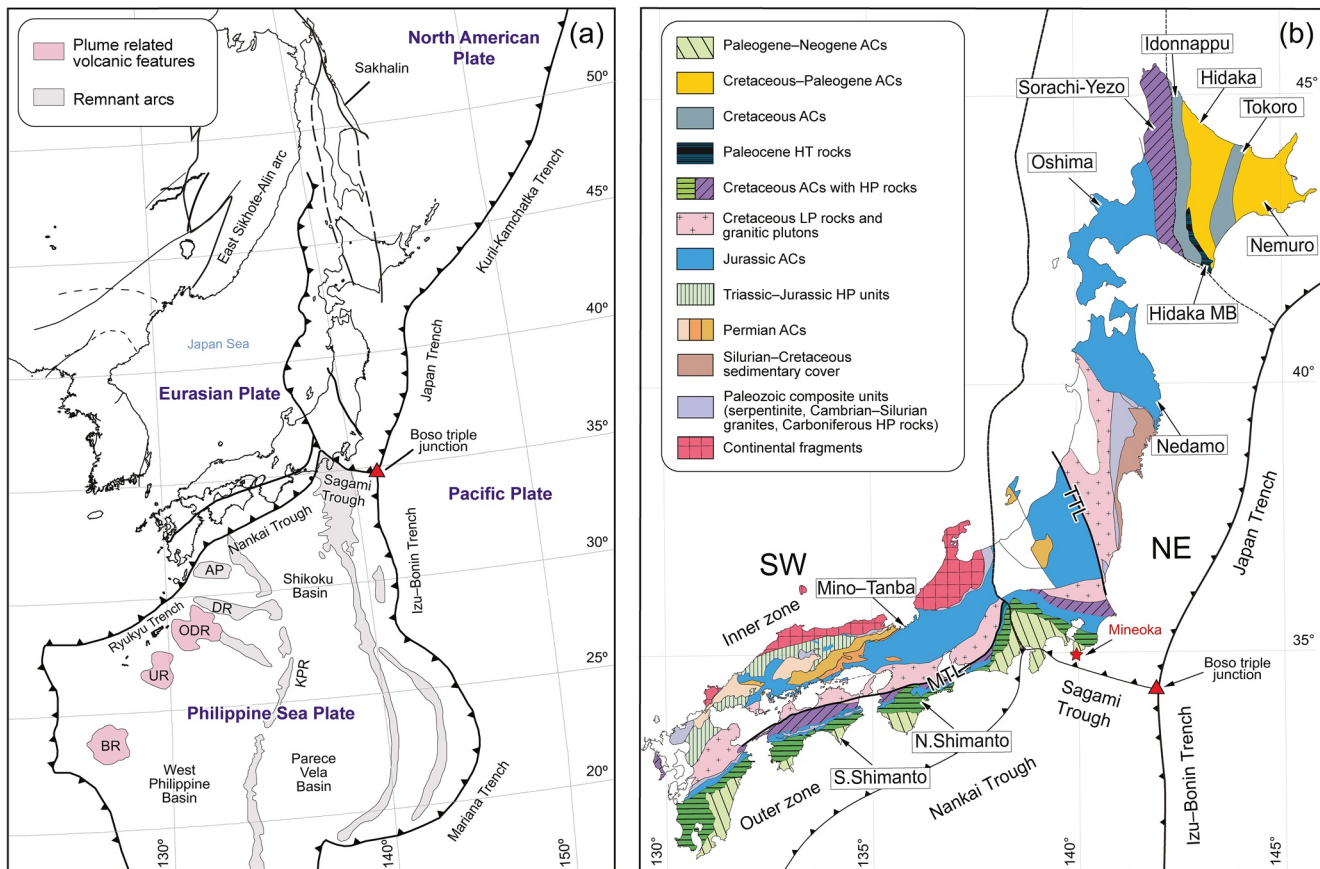


Figure 1. (a) Tectonic map of oceanic plates in the East Asia and location of the Mineoka Ophiolite Mélange (modified from Harada et al., 2021; Ishiwatari et al., 2016; Tsujimori & Liou, 2005). AP- Amami Plateau; DR- Daito Ridge; ODR- Oki Daito Ridge; UR- Urdaneta Ridge; BR-Benham Rise; KPR- Kyushu-Palau Ridge. (b) Geotectonic subdivision of the Japanese Islands (modified after Pastor-Galán et al., 2021).

continues to the Miura Peninsula, the Kobotoke Mountains, and ends in the eastern Shizuoka City. It has been referred to as the “Circum-Izu Massif Serpentinite Belt” (Arai, 1994; Arai & Ishida, 1987) and currently as the Mineoka–Setogawa Ophiolitic Mélange (Ishiwatari et al., 2016). The origin and provenance of the MOM are controversial with different hypotheses, including (1) fragments of the abyssal peridotite beneath the Shikoku Basin in the Philippine Sea Plate and uplifted during the collision (Arai, 1991); (2) ophiolite serpentinites are upwelled seamount serpentinites of IBM arcs by occurrence mode similarities with IBM seamounts (Fujioka et al., 1995); (3) an independent “Mineoka Plate” due to the discrepancy of igneous rock ages and pelagic covers in the “Mineoka Belt” and the Pacific, and Philippine Sea Plate (Hirano et al., 2003; Mori et al., 2011; Ogawa & Takahashi, 2004; Ogawa & Taniguchi, 1988), which would be the origin of the MOM. These hypotheses are mainly based on their lithostratigraphic features, structures developed during accretion, geochronology of igneous and metamorphic rocks, and their geochemical signatures. To fully understand the origin and history of the MOM, spatial and kinematic constraints and its integrity with plate tectonic reconstructions are necessary.

In this paper, we present the new paleomagnetic data from pillow basalts and dolerite dikes from the MOM, and the subsequent kinematic evolution until its emplacement, and its link with the Japanese subduction system and the neighboring plates.

2. Geological Setting

2.1. Overview of the Oceanic Plates of the Western Pacific

Oceanic crustal activity around Japan is controlled by the subduction, and interaction of the Pacific, Eurasian, North American, Philippine Sea, and smaller plates and blocks (Okhotsk, Amur, Kuril, etc.), and other already vanished oceanic plates (e.g., Izanagi) (Figure 1a).

2.1.1. Pacific Plate

The Pacific Plate is a complete oceanic plate with Jurassic to present day oceanic crust and a large number of seamounts and oceanic islands, where many of them plume derived (e.g., Hirano et al., 2003; Ichiyama et al., 2008; Tatsumi et al., 2000). The plate was generated in the Early Jurassic (~190 Ma), in a triple junction between the presently extinct Farallon, Izanagi, and Phoenix plates (e.g., Boschman & van Hinsbergen, 2016; Seton et al., 2012), where the growth accelerated during the Aptian (Cretaceous) (e.g., Engebretson et al., 1985; Wright et al., 2016). Spreading began along the E–W trending Kula–Pacific and NE–SW trending Kula–Farallon mid-ocean ridges (e.g., Whittaker et al., 2007; Woods & Davies, 1982) and the Kula–Pacific mid-ocean ridge continued until ~40 Ma, then Kula Plate almost completely subducted beneath the North American Plate (Fuston & Wu, 2020; Lonsdale, 1988; Müller et al., 2016). The subduction of the Pacific–Farallon plates led to a complex system that included several Farallon heired microplates (e.g., Juan de Fuca, Vancouver, Cocos, Nazca), ridge jumping, propagating (Seton et al., 2012), and fragmental subduction of the dominant part beneath the North and South America continuing until the present day (e.g., Sigloch & Mihalynuk, 2013).

In the NW Pacific, at ~85 Ma, an intra-oceanic arc (Nemuro–Olyutorsky) formed above a southeast dipping subduction (Domeier et al., 2017; Vaes et al., 2019). Vaes et al. (2019) suggested that this subduction initiated along the detachment fault near and parallel to the Izanagi–Pacific spreading ridge following the model shown on Vardar Ophiolites of Greece and Serbia (Maffione & van Hinsbergen, 2018). Olyutorsky arcs migrated rapidly northwards with trench roll-back, until Izanagi–Pacific ridge subduction and arrived at a similar latitude with Kamchatka by the ~50 Ma (Levashova et al., 2000) and resulted an arc-continent collision (Domeier et al., 2017; Solov'ev et al., 2011). After the collision, on the outboard side of the accreted Olyutorsky arcs, the Pacific Plate started to subduct below East Asia with a north-dipping polarity, in the back-arc lithosphere of former southward subduction, as it became easy to rupture by mantle advection of the previous subduction.

The Pacific slab, that subducted after Izanagi–Pacific ridge, is visible on mantle tomography, as a 2,500 km long, west-dipping flat slab below Japan, located in the upper mantle, and is disconnected from deeper anomalies in the lower mantle (Seton et al., 2015; van der Meer et al., 2018). However, the plate kinematics of Izanagi–Pacific ridge subduction, exact timing, and orientation of the plate boundaries are under debate with several options including: (1) strongly oblique to the Japanese coast (e.g., Maruyama et al., 1997), (2) almost parallel to it (e.g., Liu et al., 2020; Seton et al., 2015; Whittaker et al., 2007; Wu & Wu, 2019), and (3) a marginal sea closure which would not include ridge subduction below Japan (Domeier et al., 2017). Ridge subduction would have caused a slab detachment that possibly triggered a plate-driven force change and a change into the mantle flow in the area of East Asia.

The former Izanagi–Pacific spreading ridge preserved in the forearc basin of the nascent subduction zone, restored and marks the Pacific–Olyutorsky plate boundary. To the south, the Pacific Plate has steadily converged under the Philippine Sea Plate at least since 52 Ma (Figure 1a). It has formed Izu–Bonin–Mariana oceanic island arcs that extend from Honshu, Japan to Guam and a succession of magmatic episodes of subduction initiation, normal arcs, several periods of seafloor rifting and spreading from 52 to 31 Ma (Ichiyama, Ito, Tamura, & Arai, 2020; Ishizuka et al., 2013). The Neogene tectonic events of the NW Pacific include the opening of the Japan Sea, Kuril, and Komandirovsky back-arc basins of Sakhalin (e.g., Vaes et al., 2019).

2.1.2. Okhotsk Plate (North American Plate)

The Okhotsk Plate is a putative minor plate that would cover the Okhotsk Sea, Far East Russia, and NE Japan (Maruyama et al., 1997; Rodnikov et al., 2013). The origin of the Okhotsk Plate is unclear. Seno et al. (1996) suggested that it is part of the North American Plate. A group of researchers suggested that it

is an independent microplate, based on its different kinematics from the North American Plate (e.g., Apel et al., 2006).

2.1.3. Philippine Sea Plate

The Philippine Sea Plate is an oceanic plate surrounded by the Pacific and Eurasia plates to the east and west and by the Sunda, Indo-Australian, and Caroline plates to the south (Figure 1a; Seno & Maruyama, 1984; Wu et al., 2016). The plate boundaries are all convergent: Along its western margin, the Philippine Sea Plate is subducting beneath the Eurasian Plate, at the Philippine, Manila, Ryukyu trenches, and the Nankai and Sagami trough to the north. On its eastern margin, it overrides the Pacific Plate at the Izu–Bonin–Mariana, Yap, and Palau trenches (e.g., Wang et al., 2008). Absolute plate motion of the present Philippine Sea Plate is ~6–11 cm/yr, to the WNW, quicker than that of the Eurasia, and comparable to the abutting Pacific and Caroline Plate motions (9.5–11 cm/yr) (Argus et al., 2011; DeMets et al., 2010).

The inception of the Philippine Sea Plate is enigmatic. Ishizuka et al. (2013) and Wu et al. (2016) proposed that the plate originated above an active plume either Oki-Daito or Manus. The origin of “Oki-Daito plume” at 52–50 Ma and the prospective inception of the Philippine Sea Plate could be linked to the Izanagi–Pacific ridge subduction and detachment that produced a subsequent plate-reorganization with a regional mantle flow change (Lallemand, 2016; Seton et al., 2015; Wessel et al., 2015), with the subduction initiation of the dense Pacific lithosphere along the transform fault system.

The Philippine Sea Plate consists of three oceanic basins, with rises and plateaus, fracture zones, spreading ridges, and several oceanic arcs and arc-relics with ages ranging from Late Cretaceous to Neogene. The oceanic basins are younging eastward (e.g., Lallemand, 2016). The opening of the West Philippine Basin occurred between 55 and 26 Ma (Deschamps & Lallemand, 2002; Sasaki et al., 2014). After the spreading of the West Philippine Basin, the Shikoku and Parece-Vela basins rifted from ~29 Ma as a “twin back-arc” opening, possibly triggered by slab rollback of the Pacific Plate accompanied by the rotation of the Philippine Sea Plate (Sdrolias et al., 2004). The N–S oriented, Kyushu–Palau Ridge separates these two basins (Figure 1a; Tokuyama, 1986). The Mariana Trough has spread as a back-arc basin with rates of 20 mm/yr in the north, to 40 mm/yr in the south from ~8 Ma (Asada et al., 2007; Deschamps et al., 2005).

The plate also includes leftovers of previous island arcs and plume magmatism (Figure 1a). To the north of the Western Philippine Basin comprised Cretaceous arc remnants (Amami Plateau, Oki, and Daito Ridges) and now get trapped in the Philippine Sea Plate (Hickey-Vargas, 2005; Ishizuka & Yuasa, 2007). They are separated by oceanic basins and now subducting beneath the Ryukyu Ridge (Nishizawa et al., 2014; Tokuyama, 2007). Plume-derived bathymetric highs to the south (Benham Rise, Urdaneta Plateau, Oki-Daito Rise), exhibit a systematic age progression from 51 to 36 Ma (Ishizuka et al., 2013; Nishizawa et al., 2014). During the Miocene (20–17 Ma), the Philippine Sea Plate collided with the Ryukyu continental margin, SW Japan (e.g., Seno & Maruyama, 1984).

Previous paleomagnetic studies of the Philippine Sea Plate generally show that it is traveled northward ~20° (>2,000 km) (e.g., Hall, Ali, Anderson, et al., 1995; Haston & Fuller, 1991; Larson et al., 1975). The majority of northward movement occurred before 25 Ma, then stabilized after 15 Ma. According to the paleomagnetic declinations (e.g., Hall, Ali, Anderson, Baker, et al., 1995; Haston & Fuller, 1991; Koyama, 1991), the plate has rotated up to ~105° in a clockwise sense. Offshore paleomagnetic studies from the Ocean Drilling Program (ODP) in the West Philippine Basin and Benham Rise, also support a deceleration of Philippine Sea motions toward the north, since 20 Ma (Louden, 1977; Richter & Ali, 2015).

Paleomagnetic records suggest 90° clockwise rotation with a mean angular velocity of 2.57°/m.y. around the Euler pole at 23°N, 162° E before 25 Ma, which is compatible with the motion of the Japanese Islands (Yamazaki et al., 2010). The collision of the Izu–Bonin–Mariana arcs with the SW Japan arcs is estimated to have commenced at about 15 Ma, and there has been no significant location change since then (e.g., Amano, 1991; Takahashi & Saito, 1997). Another model proposed that the Philippine Sea Plate rotated clockwise by 34° between 25 and 5 Ma, remained stable between 40 and 25 Ma (Hall, Ali, Anderson, et al., 1995; Hall, Ali, Anderson, Baker, et al., 1995), constraining from the paleomagnetic data from eastern Indonesia. Some studies argued that the rotation occurred on a local scale rather than an entire plate.

2.1.4. Vanished East Asian Sea Plate(s)

In the continued history of the Pacific Ocean subduction, many plates have been completely consumed. Wu et al. (2016) reconstructed and mapped the slabs below East Asia, including the still existing Pacific, Indian, and Philippine Sea plates. Vertical tomographic cross-sections revealed a swath of anomalies from SW Japan to New Zealand that they inferred as slabs and called them “East Asian Sea” slabs. Following Wu et al. (2016), the Northern East Asian Sea was surrounded by the proto-South China Sea and the Ryukyu margin on its western and northern margins and probably had a similar motion to the Eurasian Plate. During the Late Cretaceous time (~85 Ma), Southeast China experienced an arc magmatism gap (Li, 2000; Li et al., 2014), and the convergent margin transitioned to an extensional setting along the East Asia (Liu et al., 2014). A series of oceanic basins opened in, at least, two phases along east and south China (Deschamps & Lallemand, 2002; Ren et al., 2002; Zahirovic et al., 2014). The formation of the East Asian Sea was possibly related with these rifts, either as a back-arc basin of the proto-South China Sea or as marginal seas, as it has abutted the proto-South China Sea. The origin of the East Asian Sea could have linked to the slab rollback, retreat, or jumping of the paleo-Pacific subduction zone beneath SE China (Zhou & Li, 2000). The East Asian Sea Plate probably subducted to the southeast beneath the northwest moving Philippine Sea Plate, to the north under the Pacific. In the literature we found several plate names referring to sections or the whole East Asian Sea slab: For example, proto-Philippine Sea Plate (Hall & Spakman, 2002; Lallemand, 2016), North New Guinea Plate (Seno, 1984), Heike Plate (Yamaji & Yoshida, 1998), and Mineoka Plate (e.g., Hirano et al., 2003). A short-lived hypothetical Heike Plate detached from the Pacific at about 19 Ma followed by its slab roll back and have caused mantle upwelling that is responsible for the widespread 16–15 Ma magmatism in the SW Japan. The plate was completely demised by 15 Ma (Yamaji & Yoshida, 1998).

The putative Mineoka Plate would have formed in the Late Cretaceous and was totally consumed during the Oligocene and probably subducted beneath the northern margin of the Philippine Sea Plate, while Pacific Plate moved northwards. It could have bordered by subduction zone or transform fault with the Pacific Plate. When the Pacific changed its motion, subduction beneath the Mineoka possibly initiated, and the small plate could have been experienced arc volcanism (Mori et al., 2011) at least until 23 Ma based on bulk-rock Ar–Ar age (Hirano et al., 2003). In the early Miocene, seamount-like alkaline basalt could have erupted in the Mineoka Plate, after its spreading cessation.

2.2. Overview of the Japanese Islands

The present-day Japan Arc is a 3,000 km long chain of islands located at present on the junctions of four different plates: Eurasian (Amur), Pacific, North American (Okhotsk), and Philippine Sea plates (Figure 1a). The Pacific Plate is subducting beneath the NE Japan and the Philippine Sea Plate at a rate of 10 cm/yr, whereas the Philippine Sea Plate is subducting beneath the SW Japan along the Nankai Trough and the Ryukyu Trench of SW Japan from SE to NW with a 4 cm/yr rate (e.g., DeMets et al., 2010). The particular present-day tectonic setting of Japan is the result of a protracted history of subduction, obduction, and collision/subduction of minor arcs and seamounts since the late Ordovician (e.g., Maruyama et al., 1997; Maruyama & Seno, 1986; Isozaki, 1996; Isozaki et al., 2010). The geotectonic units of present-day Japan arc are divided into SW and NE Japan by the Tanakura Tectonic Line (TTL: Figure 1b). SW Japan is characterized by a series of orogen-parallel accretionary complexes; the Median Tectonic Line (MTL) further separate the inner and outer zones. The overall structure is a pile of subhorizontal nappes, which older sheets usually occupy the upper structural positions. Voluminous calc-alkaline granitic batholiths intruded the nappe structure in Cretaceous time, gently folding them to form synform-antiform structures. Cretaceous batholith in SW Japan extends to NE Japan and further to Eastern Sikhote-Alin of Far East Russia (Grebennikov et al., 2016; Jahn et al., 2015). Accretion has been, apparently, episodic at Carboniferous (Nedamo Belt), Late Permian (Akiyoshi and Ultra-Tamba), Jurassic (Mino-Tamba, North Kitakami, Oshima), Late Cretaceous–Neogene (Shimanto, Idonnappu and Hidaka) (e.g., Isozaki et al., 2010). The Mineoka Ophiolite Mélange (MOM, a. k.a. Mineoka–Setogawa ophiolite) is located in the Shimanto Belt.

The Shimanto Belt is developed along the outer zones of SW Japan (Figure 1b). It includes autochthonous turbidites, accreted cherts, and pillow basalts. Some accretionary complexes in Hokkaido, such as Idonnappu, and Hidaka belts, are contemporaneous to the Shimanto Belt, suggesting a coeval accretion

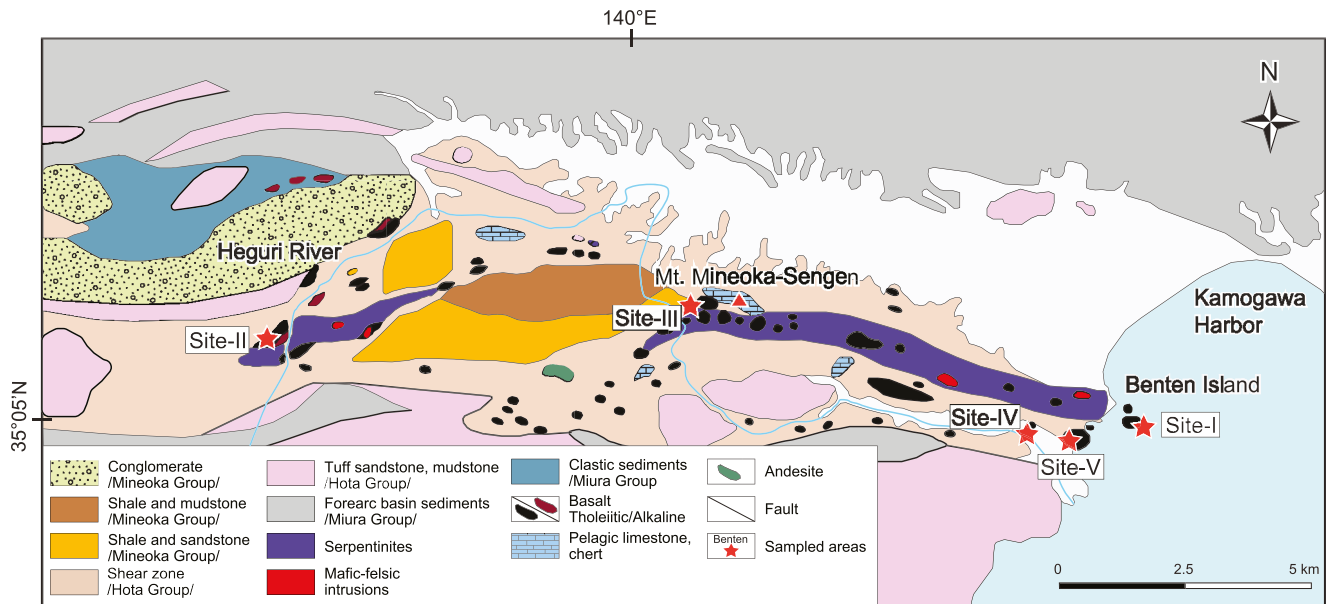


Figure 2. Simplified geological map of the Mineoka ophiolite. Sampling site names: Site I–BNT, Site II–HGR, Site III–QWS, Site IV–SNY, Site V–KM.

at along >2,000 km long, same convergent margin (e.g., Kimura et al., 2016). The Shimanto Belt has been subdivided into a northern and southern unit. The northern unit is an Early to Late Cretaceous in age, whereas the southern unit is an Eocene to early Miocene, and has abundant allochthonous chert and basalt relative to the older unit (Taira, 1988). The MOM occurs in the southern unit. The Shimanto Belt includes fragments of the Izanagi Plate ($\geq \sim 85$ Ma), Kula Plate (85–65 Ma), Pacific Plate (65–20 Ma), and Philippine Sea Plate since the Miocene. The first three plates were separated by extensional and ridge subduction may be involved during the different geological processes. It has been suggested that the Shimanto Belt recorded an Eocene (50–40 Ma) enhanced thermal event, interpreted as the consequence of ridge subduction (e.g., Hara & Kimura, 2008; Hasebe & Tagami, 2001). However, there is a lack of geological criteria to determine whether ridge subduction occurred, and if so, which pair of plates bounded such ridge.

2.3. Geology of the Mineoka Ophiolite Mélange (MOM)

The MOM is an E–W-trending, 5 km wide and fault bounded outcrop located in the Boso Peninsula in Chiba prefecture, Japan. The rocks crop out from Kamogawa Harbor east of Boso Peninsula to Hota Beach, to the west of the peninsula (Figure 1b; Ogawa & Taniguchi, 1988). The MOM continues to the Miura Peninsula, to the Kobotoke Mountains, and ends in eastern Shizuoka City, along the north of the Izu Peninsula (Figure 1b; e.g., Ichiyama et al., 2017). The MOM includes abundant serpentinite, gabbro, diorite, amphibolite, basaltic rocks, ultramafic rocks, and serpentinitized harzburgite in association with serpentine sandstone and conglomerate (cf. Arai et al., 1991). The overall highly fragmental 'mélange'-like occurrence may be related to its emplacement mechanism at a trench–trench–trench triple junction (Mori & Ogawa, 2005). The fragments of oceanic lithosphere rock and metamorphic rocks crop out as tens to hundreds of meters sized blocks within a serpentinite distributed all over the MOM (Figure 2). Blocks show various shapes (oblate, prolate, and spherical) and are bounded by discrete fault zones (Ogawa & Takahashi, 2004). Serpentinites occur not only as a matrix but also as discrete blocks and are composed mostly of lizardite, chrysotile (Ogawa et al., 2009). The fragments of oceanic crustal rock consist of pillow basalts, sheeted dolerite dikes, plutonic rocks, with minor pelagic to hemipelagic sedimentary rocks. Pelagic and hemipelagic sedimentary rocks show biostratigraphic ages ranging from Late Albian radiolarian fossils in the Yo-oka Beach of Kamogawa Harbor (Ogawa & Sashida, 2005), and from Paleocene to Miocene elsewhere (Mohiuddin & Ogawa, 1998; Takahashi, 1994).

The most abundant rock in the MOM is basalt with different degrees of alteration, which occurs in blocks ranging from 100 m to 1 km in diameter, mainly tholeiitic in composition with minor alkaline basalts rarely

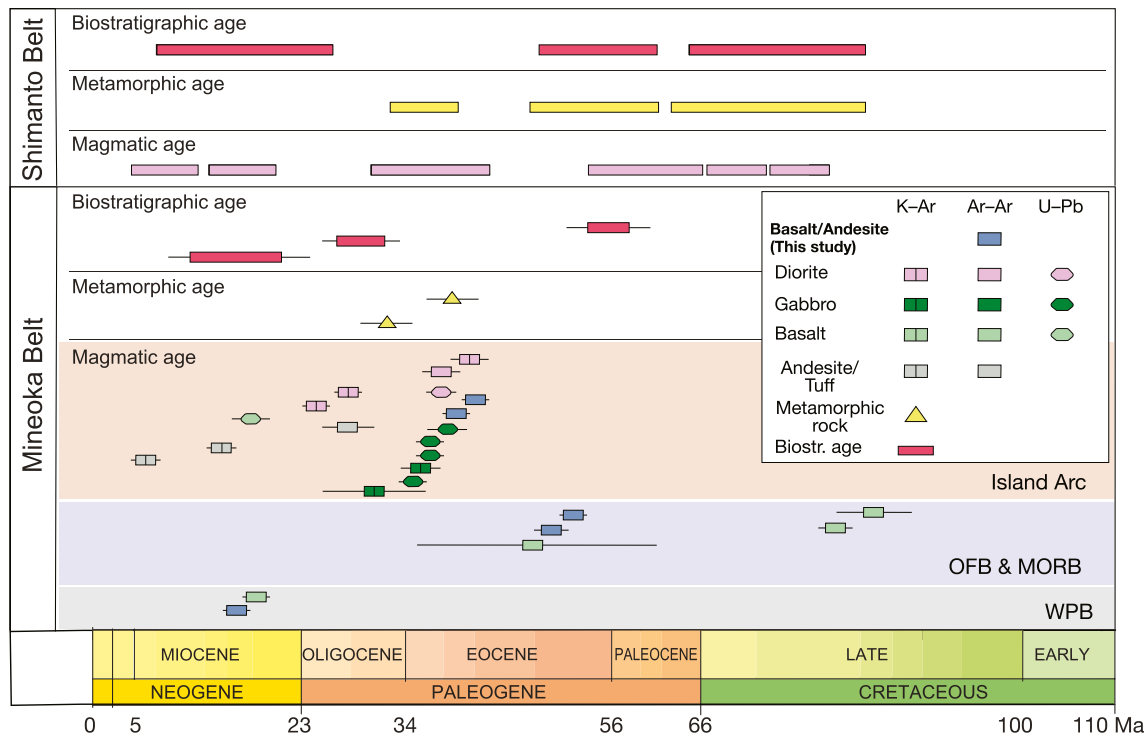


Figure 3. Summary of geochronological results of the current and previous study in the Mineoka and Shimanto Belts. References used for Mineoka Belt: Enomoto et al., 2018; Hirano & Okuzawa, 2002; Hirano et al., 2003; Ichiyama et al., 2017; Mori et al., 2011. References used for Shimanto Belt: Aoki et al., 2007; Aoki et al., 2011; Hara & Kimura, 2008; Hasebe & Tagami, 2001; Itaya et al., 2011; Raimbourg et al., 2017; Sakai, 1988.

intruded by dolerite dikes (Ogawa & Taniguchi, 1988). Tholeiitic basalts erupted between the Cretaceous and Eocene, whereas alkaline basalts erupted from Miocene times (Figure 3; Hirano et al., 2003). Chemically, Cretaceous (85–80 Ma) pillow basalts show Mid-Ocean Ridge Basalt (MORB) and Back-Arc Basin Basalt affinities (BABB) (Figure 4) (Hirano et al., 2003; Ogawa & Takahashi, 2004). Eocene (49–47 Ma) basalts and dolerites vary between Island Arc Tholeiite (IAT), MORB, and BABB (Figure 4) (Ogawa & Takahashi, 2004; Ogawa et al., 2009). The youngest alkaline basalts (25–16 Ma) show typical characteristics of Within Plate Basalts (WPB) (Figure 4) (Hirano et al., 2003). Geochemical data by previous studies are available in Table S1.

Diorites and gabbros associated with the MOM yielded 41–24 Ma (Figure 3) and have been interpreted as island arc derived (Figure 4) (Hirano et al., 2003; Mori et al., 2011; Ogawa et al., 2009). These ages are consistent with 28.6 Ma high-Mg andesite (Mori et al., 2011). The youngest ages reported from the MOM are 19 Ma from andesite-tuff breccia and 5.8 Ma from pumice (Enomoto et al., 2018; Mori et al., 2011). Some sections of the MOM experienced greenschist to amphibolite facies and retrograde epidote-amphibolite facies of metamorphism, observed in four metamorphic blocks composed of metabasite and clastic schist with mineral assemblage: quartz, feldspar, muscovite, Mn-rich garnet, piemontite, aegirine-augite (Hiroi et al., 1992). This assemblage implies the accumulation of sediments such as chert terrigenous sandstone, probably deposited near the trench, proximal to the continent (Hiroi et al., 1992; Mori et al., 2011). Greenschist and amphibolite-facies metamorphic rocks undergo their metamorphism between 39.2 and 33.1 Ma (hornblende K–Ar age; Mori et al., 2011). Ultramafic masses in the MOM are characterized by the presence of chromian-spinel or plagioclase-bearing peridotite; harzburgite is predominant over dunite in the peridotitic blocks (Arai, 2018; Arai & Uchida, 1978). Formation of plagioclase-bearing peridotite is attributed to the melt infiltration of residual peridotite and melt mantle interaction at shallow depth as a product of the reaction between peridotite and melt flow (e.g., Dick, 1989; Saper & Liang, 2014).

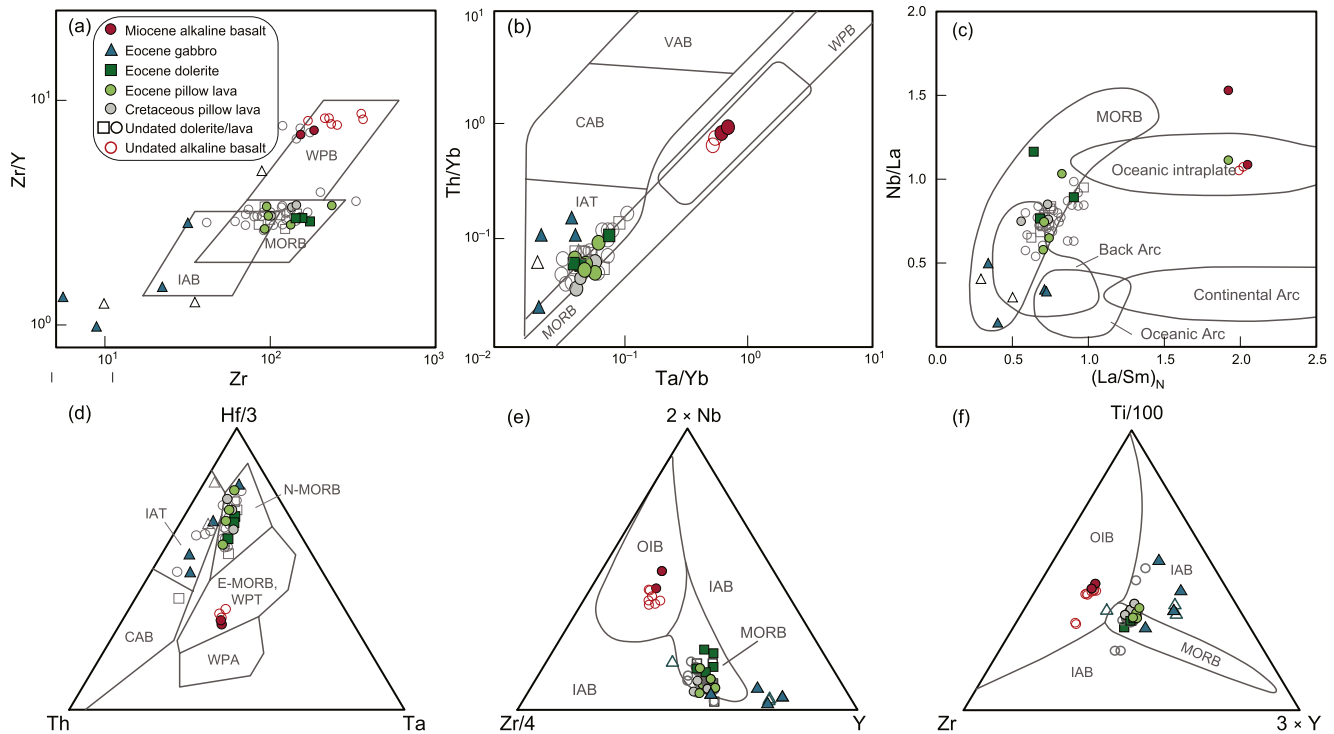


Figure 4. Tectono-magmatic discrimination diagrams for the mafic rocks of the Mineoka Ophiolite Mélange. (a) Pearce & Norry, 1979; (b) Pearce, 2003; (c) John & Schenk, 2003; (d) Wood, 1980 (e), (f) Vermeesch, 2006a, 2006b. N-MORB–normal mid-ocean ridge basalt; E-MORB–enriched mid-ocean ridge basalt; OIB–ocean island basalt; OIA–ocean island alkaline; WPB–within plate basalt; IAB–island arc basalt; CAB–calc-alkaline basalt. Data compiled from Hirano & Okuzawa, 2002; Hirano et al., 2003; Mori et al., 2011; Ogawa et al., 2009.

3. Sampling Sites and Lithological Variations

3.1. Sampling Sites

We drilled a total of 113 cores of basalts and dolerites with a petrol engine drill in five sites in Mt. Mineoka-Sengen-Kamogawa area (Figure 2; Table 1) for paleomagnetic analysis. We also have collected four samples (BM08SG2, BM25BT3, BM981107-03, and BM010422-07) from this sites for bulk-rock $^{40}\text{Ar}/^{39}\text{Ar}$ age dating (Figure 2 and Table 1). The geochemical signatures of these samples were referred in the previous studies (e.g., Hirano et al., 2003; Mori et al., 2011). For comparison, one additional sample (BM000513-06) were collected from a location ~9 km west of the Mt. Mineoka-Sengen-Kamogawa area for age dating.

Site-I: BNT (Benten) – The site is located at the Benten Island, and represents the easternmost outcrop of the Mineoka ophiolite (Figure 2). It consists of pillow basalts and dolerite sheeted dikes. Pillow basalts are varying: Black-colored IAT in the northeast and red-gray basalts in the north and west (Hirano et al., 2003; Ogawa & Takahashi, 2004). Dolerite dikes are coarse-grained with the general strike of N 60–80°W and

Table 1
Paleomagnetic Sampling Sites From the Mineoka Ophiolite Mélange

Sampling sites	Coordinate		Age, Ma	Lithology	Mean azimuth		Reference
	Latitude, N	Longitude, E			Dip direction	Dip	
Site-I (BNT)	35°05'26"	140°06'35"	~50	Sheeted dikes	220	15	Hirano et al. (2003), This study
Site-II (HGR)	35°06'14"	139°55'50"	~16	Alkaline basalt	72.9	16.2	Hirano et al. (2003), This study
Site-III (QWS)	35°06'40"	140°01'05"	~50	Tholeiitic basalt	357	19.3	This study
Site-IV (SNY)	35°05'16"	140°05'52"	~85	Tholeiitic basalt	86.2	57.6	Mori et al. (2011)
Site-V (KM)	35°05'10"	140°05'57"	~85	Tholeiitic basalt			Mori et al. (2011)

steep dip to the south were intruded by fine-grained dolerite dikes and dike swarms with chilled margins. Together they are faulted along with the steep dip, dike-parallel oblique faults, and cut by hydrothermal veins with various orientations. Tholeiitic pillow basalts erupted at 49 ± 13 Ma (bulk-rock $^{40}\text{Ar}/^{39}\text{Ar}$ plateau age) (Figure 3; Hirano et al., 2003) and show MORB-like geochemical signature. We collected 29 cores from the sheeted dikes for net tectonic analysis from two different areas with slightly different strike and dip, and one sample (BM25T3) for Ar–Ar analysis.

Site-II: HGR (Heguri-naka)– It is located to the west of Mt. Mineoka-Sengen (Figure 2), along the distinct fault zone bounded serpentinite bodies. It consists of alkali-basalts with olivine and pyroxene phenocrysts. It occurs as sheet flows and vesicular pillow basalt and sections of basaltic clastic sandstone, conglomerate, glauconitic shale, micritic limestone, and siliceous shale overlie it. It extruded at 19.62 ± 0.90 Ma [MSWD = 0.93] (bulk-rock $^{40}\text{Ar}/^{39}\text{Ar}$ plateau age; Hirano & Okuzawa, 2002) and characterized by WPB geochemistry. We collected 34 core samples from a small size river outcrop with two distinct lithologies: Gray basalts and red basalts and one sample (BM010422-07) from red basalts for age dating.

Site-III: QWS (Quarry Western Sengen) – Outcrop of 100 m long pillow basalt block is located 500 m to the northwest from Mt. Mineoka-Sengen, along the Heguri River (Figure 2). Pillow basalts are surrounded by a serpentinite matrix with shearing and brecciation zones between both basalt and serpentinite (Ogawa et al., 2009). We sampled 10 cores from individual pillows at different stratigraphic levels and one sample (BM08SG2) from basalt and one andesitic sample (BM981107-03) from the nearest outcrop for age dating.

Site-IV: SNY (Shinyashiki) – A 300 m wide, large tholeiitic pillow basalt outcrop is located to the south of Benten Island (Figure 2). They are yielded a plateau age of 85.0 ± 3.9 Ma [MSWD = 1.4] and 80.6 ± 1.7 Ma [MSWD = 1.1] (Mori et al., 2011), and exhibit MORB and BABB geochemical pattern. In the middle of the stratigraphic sequence, pillow basalts are intercalated with massive flows and are cut by several sheeted dolerite dikes. The sequence has a moderate to steep dip to the SE. Pillows are mainly several tens of centimeters and rarely up to 1 m in size. Fault, mineral precipitation, and veining in this area are subdivided into three phases (Takahashi et al., 2003). 40 cores have been collected from basaltic outcrops.

Site-V: KM (Kamogawa) – Pillow basalt outcrops in the Kamogawa Harbor. Although, they referred as part of the Site-IV, they occurred as an independent outcrop (Figure 2). 10 core samples have been collected from the site.

3.2. Lithological Variations

The investigated samples in the Mt. Mineoka-Sengen–Kamogawa are lithologically grouped in tholeiitic basalts, alkaline basalts and dolerite dikes. In this study, petrographical observations were performed on four age-dated samples from the Mt. Mineoka-Sengen–Kamogawa. Although these samples were affected partially by secondary alteration, primary igneous textures of these rocks are well preserved.

3.2.1. Tholeiitic Basalts

Pillow basalts from the Site-I and Site-V are tholeiitic. They display commonly a variolitic texture (Figures 5a–5c), characterized by the random orientation of plagioclase and some of them exhibit aphyric, hypocrystalline, amygdaloidal textures. Their groundmasses consist mainly of plagioclase laths (~0.5–1 mm in length) with clinopyroxene (0.2–0.5 mm in size) and olivine (0.2–0.5 mm in size), where they build up ~90% of all phases. Plagioclases are partially sericitized. Magnetite occurs as an accessory mineral (Figure 5a). The secondary minerals are chlorite, calcite, and rare pumpellyite (Figures 5b and 5c). Partially altered olivine is more abundant phenocryst in pillow basalts from the Site-III. Some samples from the Site-I, contains calcite vein (Figure 5d), and clinopyroxene grains are replaced by a chlorite.

3.2.2. Alkaline Basalts

Alkaline basalt (Figure 5e) from the Site-II contains mainly phenocrystic clinopyroxene, olivine (pseudomorph), and plagioclase. Clinopyroxene occurs as prismatic phenocrysts (0.5–3 mm in size), with a clear cleavage. Olivine is completely altered to chlorite. Minor secondary epidote occurs as fillings of amygdaloids. Groundmass (~80%) consists of plagioclase, volcanic glasses, and secondary minerals.

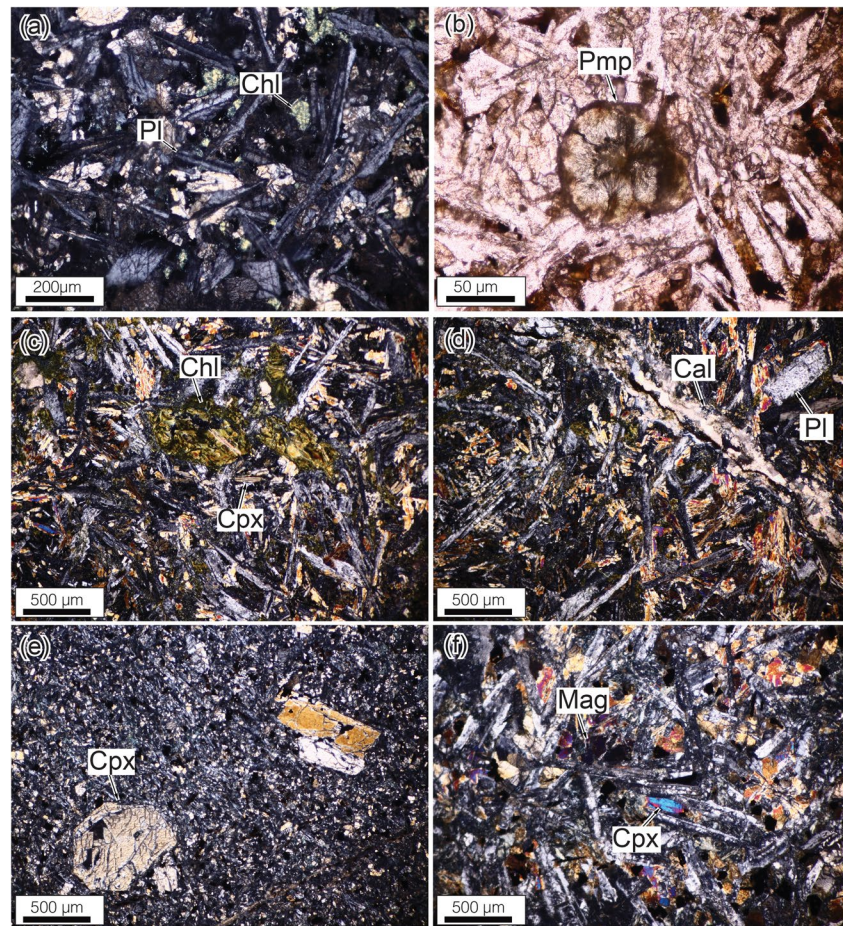


Figure 5. Photomicrographs of representative constituents from the Mineoka Ophiolite Mélange. a, c–f were taken in crossed polarized light, and b was taken in plane polarized light (a), (b) Tholeiitic basalt from Site V, and (c) Site III, (d) Site (i) (e) Alkaline basalt from Site II. (f) Sheeted dike from Site (i) Cpx–clinopyroxene, Chl–chlorite, Pmp–pumpellyite, Pl–plagioclase, Cal–calcite, Mag–magnetite.

3.2.3. Dolerite

The sheeted dikes from the Site-I consists mainly of calcic plagioclase, clinopyroxene, and show sub-ophitic texture. Plagioclase grains (typically ~ 0.5–2 mm in size) are euhedral to subhedral (Figure 5f). Colorless clinopyroxene crystals occur in the form of euhedral to subhedral. Accessory minerals are magnetite and apatite. Mafic minerals mostly have altered to chlorite. Magnetite crystals are ranging from 0.1 to 0.3 mm in size and randomly distributed.

4. Paleomagnetism

4.1. Rock Magnetism

We investigated the magnetic remanence of the samples and characterized some of their rock magnetic properties. Magnetic remanence of the samples was probed through thermal and alternating field (AF) demagnetization. AF demagnetization was carried out using a robotic 2G-SQUID magnetometer at Utrecht University, through variable field increments (3–10 mT) up to 100 mT. Stepwise thermal demagnetization was carried through 20°C –100°C increments until it reached the complete demagnetization. Principal component analysis (Kirschvink, 1980) was used to calculate magnetic component directions from “Zijderveld” vector end-point demagnetization diagrams using the free online suite Paleomagnetism.org (Koymans et al., 2016, 2020).

Table 2
Paleomagnetic Results From the Mineoka Ophiolite Mélange

Site	<i>N</i>	<i>N</i> ₄₅	<i>Dec.</i>	<i>dDec.</i>	<i>Inc.</i>	<i>dInc.</i>	<i>k</i>	<i>a</i> ₉₅	<i>K</i>	<i>A</i> ₉₅	<i>A</i> _{95min}	<i>A</i> _{95max}
Site-I –1 (BNT)	14	12	51.94	6.19	30.09	9.65	40.67	6.89	54.26	5.95	4.44	17.14
Site-I –2 (BNT)	18	18	7.35	5.1	22.39	8.9	34.36	5.98	48.85	5	3.78	13.27
Site-II (HGR)	42	39	293.18	5.07	–31.79	7.67	22.54	4.93	23.37	4.84	2.77	8.16
Site-III (QWS)	8	7	329.48	14.53	48.69	14.53	17.8	14.7	23.92	12.6	5.51	24.07
Site-IV (SNY)	40	30	69.53	9.64	29.35	15.21	6.5	11.19	9.01	9.28	3.08	9.62
Site-V (KM)	9	9	22.79	13.25	29.61	20.81	14.29	14.1	17.3	12.74	4.98	20.54

Note. *N* = total number of analyzed samples; *N*₄₅ = number of samples used for the calculation of the mean values after filtering with a 45° cutoff. *Dec.*, *dDec.* = site mean declination and associated error; *Inc.*, *dInc.* = site mean inclination and associated error; *k* and *a*₉₅ = precision parameter and semiangle of the 95% cone of confidence around the computed site mean direction; *K* and *A*₉₅ = precision parameter and semiangle of the 95% cone of confidence around the mean virtual geomagnetic pole; *A*_{95max} and *A*_{95min} = maximum and minimum value of *A*₉₅ expected from paleosecular variation of the geomagnetic field after applying Deenen et al. (2011) criteria.

Mean directions (Table 2) were assessed using Fisher statistics of Virtual Geomagnetic Poles (VGPs) compatible with the isolated directions (ChRM). Here, the *N*-dependent *A*₉₅ envelope of Deenen et al. (2011) was used to evaluate the ChRM distribution quality and reliability. These criteria evaluate whether (1) the scatter of VGP can be straightforwardly explained by paleosecular variation (PSV) of the geomagnetic field, (2) an alternate source of scattering is present except PSV (e.g., structural problems, rotations), or (3) the scatter do not represent the PSV, which may imply that the sampled rocks represent a too short period time to average the PSV. We applied a fixed 45° cut-off to the VGP distributions of each site. Many samples showed a viscous magnetic component that is removed at low temperatures and low coercivities (100°C–180°C; 0–12 mT).

Four high-field thermomagnetic runs were analyzed in the air with an in-house-built horizontal translation-type Curie balance, that had a sensitivity of about 5×10^{-9} Am² (Mullender et al., 1993). Approximately 50–80 mg of powdered samples were placed into quartz glass sample holders and fixed with quartz wool. The samples were heated and cooled at rates of 6 and 10°C/min, respectively. Stepwise thermomagnetic runs were carried out with intermittent cooling between consecutive heating steps. With consecutive heating and cooling segments are being 150, 100, 250, 200, 400, 350, 520, 450, 620, 550, 700, and finally back to 25°C, respectively. Heating and cooling rates were 6 and 10 °C/min, respectively. One hysteresis loop was measured at room temperature with an alternating gradient force magnetometer (MicroMag Model 2,900 with 2 T magnet, Princeton Measurements Corporation, noise level 2×10^{-9} Am², P1 phenolic probe). The maximum applied field was 1 T, field increment 10 mT, and the averaging time for each measurement was 0.15 s. The saturation magnetization (*M*_s), remanent saturation magnetization (*M*_r), and coercive force (*B*_c) were determined from the hysteresis loops. These parameters were determined after correction for the paramagnetic contribution from fields.

Paleomagnetic results from each sites are described below.

Site I–Petrography, demagnetization diagrams (Figure 6), and thermomagnetic curves (Figure 7) show that the main magnetic carrier is magnetite. This site has areas with different strike and dip, which showed a slightly different paleomagnetic direction and both of them with single polarity and modest inclinations. One of the groups points roughly northwards (*Dec./Inc.* = 7.35°/22.4°, *k* = 34.36, *a*₉₅ = 5.98, *K* = 48.85, *A*₉₅ = 5) and the other with a northeastward declination (*Dec./Inc.* = 51.94°/30°, *k* = 40.67, *a*₉₅ = 6.89, *K* = 54.26, *A*₉₅ = 5.95). Shapes of the VGP and clustering are consistent with a proper averaging of the PSV (Figure 8; Table 2).

Site II–Demagnetization diagrams show variable amounts of hematite (Figure 6). However, the bulk of magnetization is carried by magnetite even in the oxidized reddish samples (e.g., HGR-32) (Figure 7). Samples of this site yield a reverse single-polarity ChRM component heading to the northwest with very shallow inclinations. The shape of the VGP is elongated (Figure 8; *Dec./Inc.* = 293.18°/–31.79°, *k* = 22.54, *a*₉₅ = 4.93, *K* = 23.37, *A*₉₅ = 4.84).

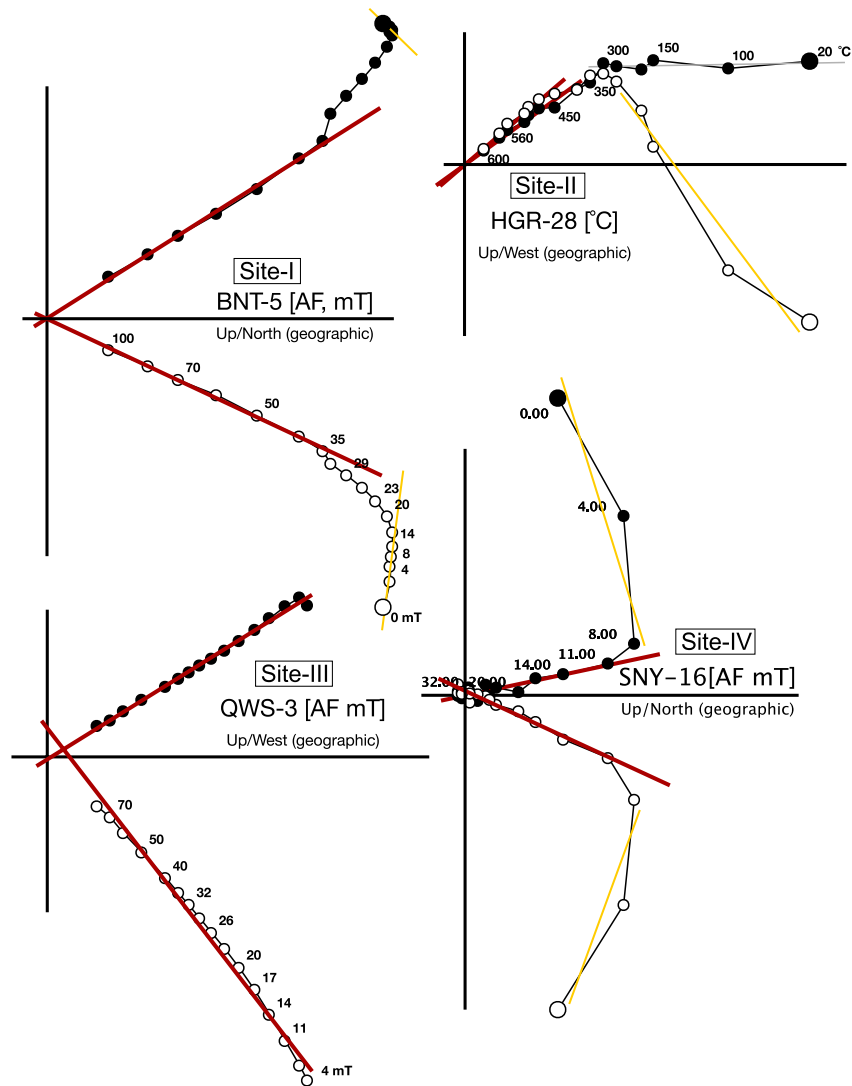


Figure 6. Orthogonal vector plots by Zijdeveld, 1967 of representative samples demagnetized using thermal (TH) and alternating field (AF) treatment. Filled dots represent projections on the horizontal and open dots represent vertical planes. Demagnetization step values are expressed in °C or in mT.

Site III–Demagnetization diagrams and the thermomagnetic curve suggest magnetite as the main carrier (Figures 6 and 7). Samples are manifested component that cluster directed to the northwest and have higher inclination ($Dec./Inc. = 329.48^\circ/48.69^\circ$, $k = 17.8$, $a_{95} = 14.70$, $K = 23.92$, $A_{95} = 12.60$). Although a limited number of core samples, shape and clustering suggest an adequate average of the PSV (Figure 8; Table 2).

Site IV–In this site we identified comparably scattered components with inclinations about 30° and declinations to the northeast ($Dec./Inc. = 69.53^\circ/29.35^\circ$, $k = 6.50$, $a_{95} = 11.19$, $K = 9.01$, $A_{95} = 9.28$) (Figure 8; Table 2).

Site V–show northwards declinations and very shallow inclinations in geographic coordinates ($Dec./Inc. = 22.7^\circ/29.6^\circ$, $k = 14.29$, $a_{95} = 14.10$, $K = 17.30$, $A_{95} = 12.74$). Once restored the pillow basalts to the paleohorizontal the inclinations fit perfectly with the Site-IV samples (Figure 8).

4.2. Net Rotation Analysis

With the net tectonic rotation analysis, we aim to determine the geometry of the seafloor spreading systems at which the oceanic crustal rocks in the MOM formed, acknowledging how limited the preserved outcrops

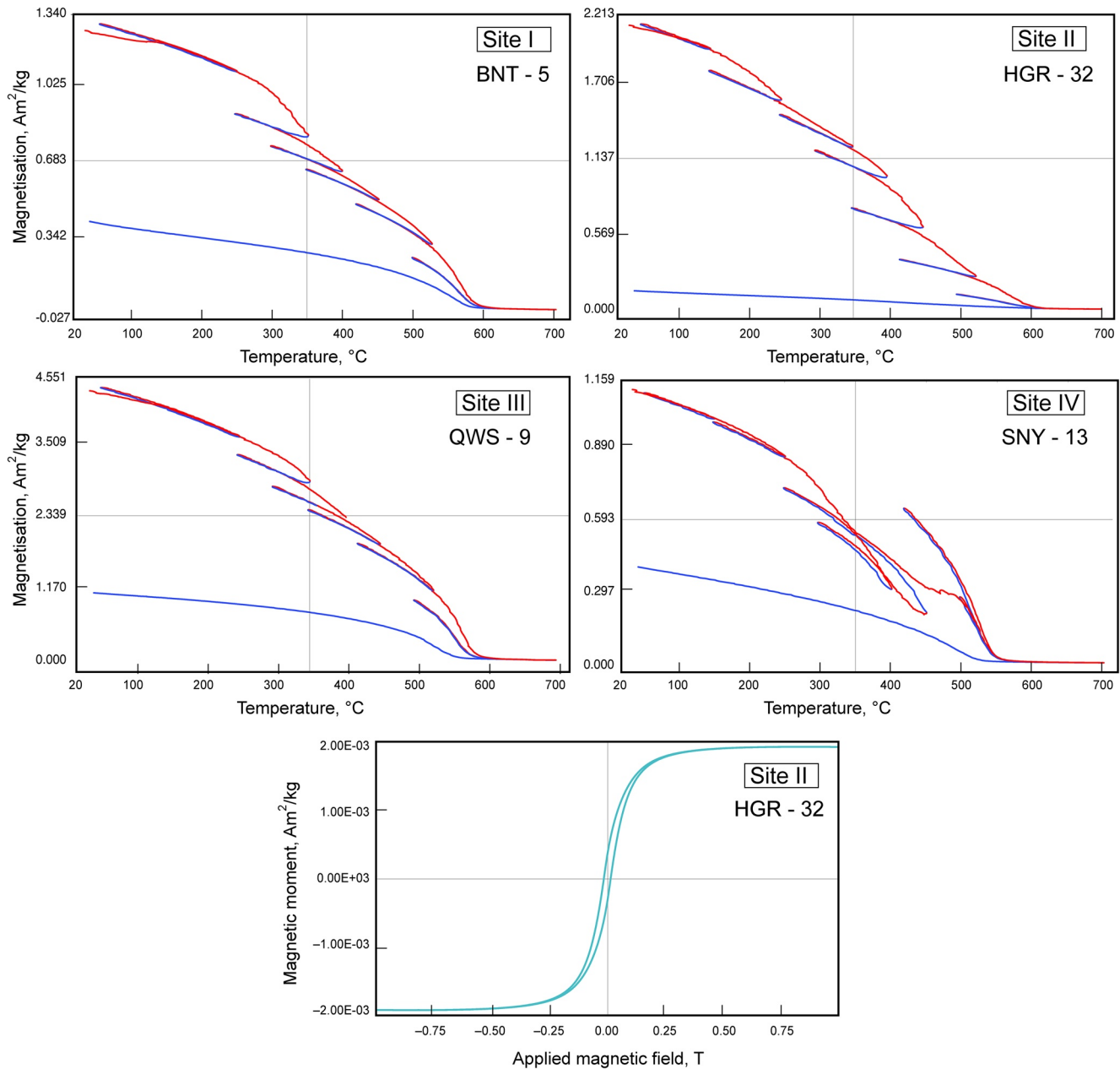


Figure 7. Thermal variation of the low-field magnetic susceptibility of representative samples from each site (red/blue represent heating/cooling); Hysteresis loop of samples from Site II.

are. From the original orientation of the spreading ridge, we will try to infer the configuration and location of the piece of the crust where the rocks of MOM belonged within the eastern Pacific Ocean mosaic of plates. The net tectonic rotation, developed by Allerton and Vine (1987), does not decompose the deformation into tilt and vertical-axis components. Instead, it calculates a single rotation that restores the sampled rock unit to its original position, and simultaneously the measured in situ remanence to its initial predeformation direction. In turn, this method requires a reference direction for the magnetic vector, which would become an assumption if we lack any paleolatitudinal constraint. The reference direction or “reference magnetization vector” is the expected paleomagnetic direction from a stable plate at a given time. In this study, we analyze the rotation relative to the geographic north assuming a geocentric axial dipole (GAD) hypothesis (i.e., the time-averaged declination of the magnetic field points toward the geographic north pole) and therefore Declination is 0°. The inclination (paleolatitude) of the reference direction has been

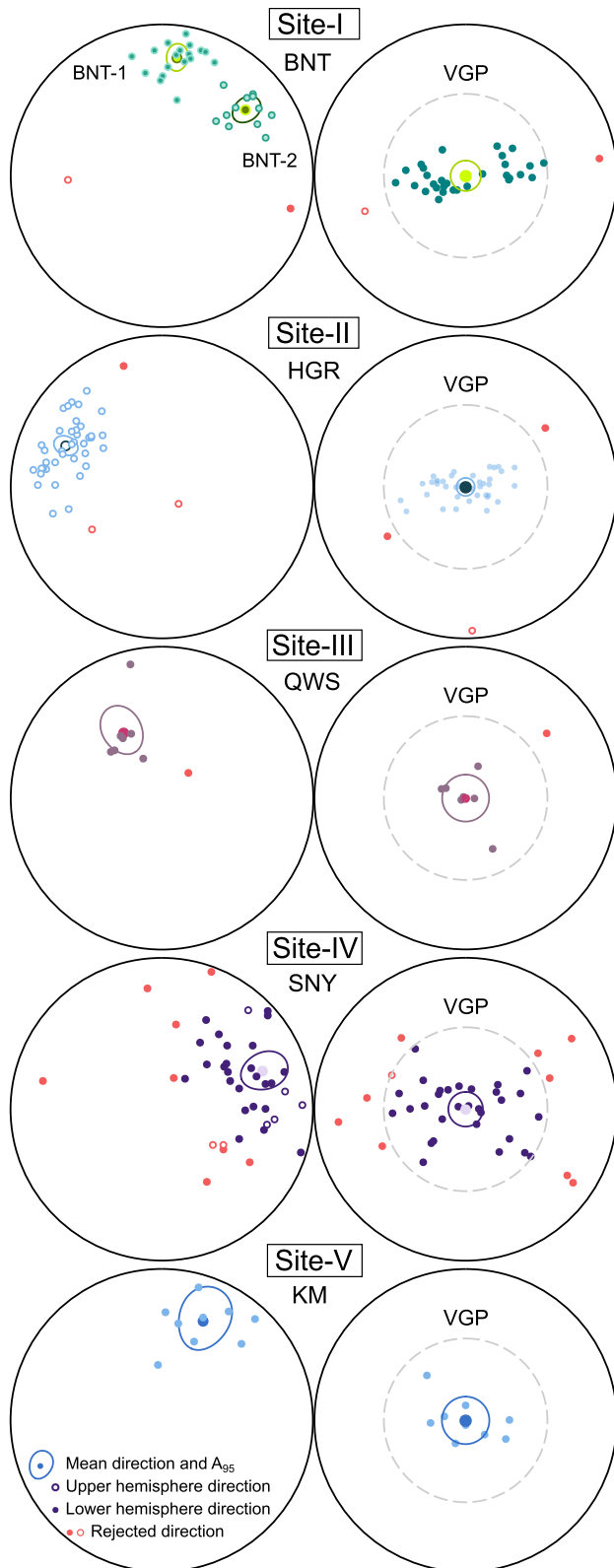


Figure 8. Equal-area projection of coercivity components from five sites of the Mineoka Ophiolite Mélange in tectonic coordinates. VGP-Virtual Geomagnetic Pole.

calculated with the results from three pillow basalt sites in this study and their comparison to the Pacific APWP extracted from paleomagnetism.org (Koymans et al., 2016). The tilt corrected mean inclination calculated from this data set, representing the inclination of the reference direction, is 52° (Figure 9). The net tectonic rotation solution set is expressed as (1) rotation axis azimuth and plunge (2) rotation magnitude and sense, and (3) initial strike of the unit. The net tectonic approach produces two possible solutions (four if we do not know the magnetic polarity at the time of acquisition) for originally vertical units like dikes. From the set of solutions, only one can be correct and it is necessary to choose. Classical selection criteria include: (1) the determined rotation must restore the units to their current position (e.g., a solution showing large rotations to produce minor movements should be rejected); (2) The rotation sense and magnitude have to be consistent with the known regional and/or local deformation pattern; (3) various sites within a relatively small region would reveal the consistent net tectonic rotation parameters (assuming local rotations are minor). If the solution is instead a single solution it means that dikes cannot be restored to a vertical position (e.g., because they did not intrude vertically). Unique solutions have no geological meaning and should be dismissed, as both the original dike orientation and the rotation parameters will only depend on the orientation of the reference direction (e.g., the initial dike orientation will always strike perpendicular to the reference direction, hence will always be E-W). Once we choose a preferred solution, we perform an iterative net tectonic rotation analysis (Koymans et al., 2016; Morris et al., 1998) to model the unreliability of the reference direction (only its inclination), the mean direction of the site, and the orientation of the dike. The webpage www.paleomagnetism.org includes a net tectonic rotation analysis package which produces at each site 75 permissible solutions per set of solutions (a total of 150 when dikes are restored to vertical).

The reference magnetization vector used in our analysis has a declination (D) of 0° . Its inclination (I) was chosen based on the expected paleolatitude of the ophiolite at the formation time of the dikes (~ 49 Ma). We used the pillow basalts results as a priori assumption on the paleolatitude of the studied ophiolite. Considering that the sampled pillow basalts' paleolatitudes from our paleomagnetic analysis perfectly match the Global Apparent Polar Wander Path (GAPWaP) adapted to the Pacific Plate (Figure 10; Koymans et al., 2016; Torsvik et al., 2012), we used the paleolatitude inferred from the GAPWaP for the sheeted dikes age (~ 49 Ma). The calculated inclination and associated error of the magnetic field, predicted for this latitudinal range is predicted to be $I = 52^\circ \pm 3^\circ$. In our analysis, we use a reference magnetization vector of $(D/I = 000^\circ/52)$. Two sets of net tectonic rotation solutions were obtained at the two different strike/dip sheeted dikes (Figure 9). The first net tectonic rotation solution is: (a) for the dikes with pole $211^\circ/25^\circ$ indicate a 50° CW rotation about shallow southwestern plunging ($182^\circ/9.8^\circ$) axis; and (b) $60^\circ/32^\circ$ with a CW rotation of 120° for the dikes with pole $235^\circ/10^\circ$. The calculated initial dike strike is consistently ESE (Table 3; Figure 9a). The second solution shows a steep northeastern plunging ($86^\circ/67^\circ$) axis with CW 67.2° rotation magnitude for dikes with poles to the dike $211^\circ/25^\circ$ and a shallower northeastern plunge ($18^\circ/32^\circ$) with CCW rotation of 103.8° for $235^\circ/10^\circ$ dikes. The initial dike orientation is ENE ($\sim 60^\circ$) (Table 3; Figure 9b). Although the net tectonic rotation analysis measures the rotation around the inclined

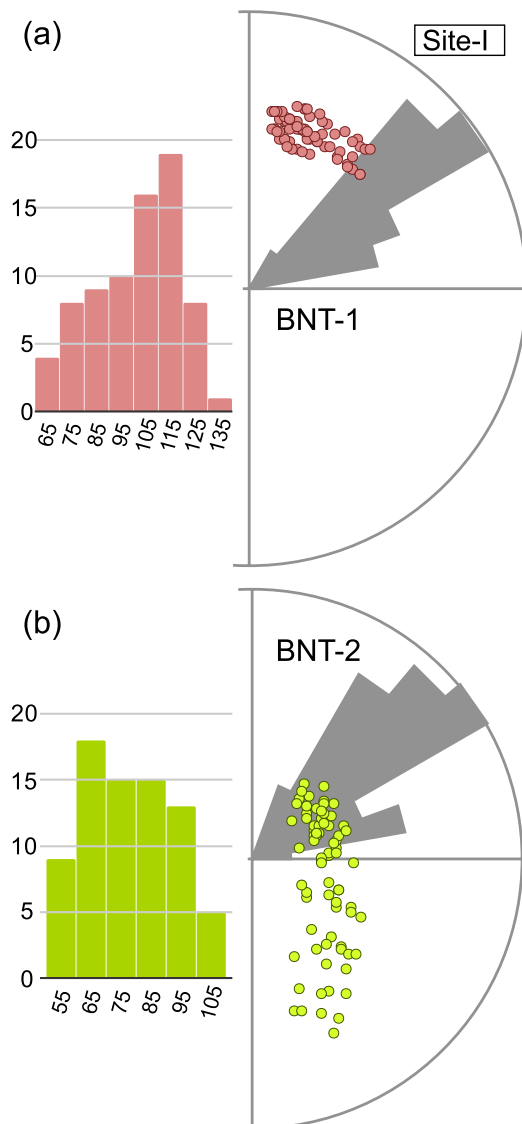


Figure 9. Rose diagram and probability histogram showing the preferred initial orientations (strike) of the sheeted dikes from the Site II (BNT) obtained after modeling of the uncertainties in the two solutions of net tectonic rotation analysis (Allerton & Vine, 1987). (a) Solution one suggests ESE ($\sim 120^\circ$) initial dike strike; and (b) solution two suggests ENE ($\sim 60^\circ$) initial dike strike.

axis, it is often possible to assume the relative magnitude of the tilt and vertical axis rotation component, constraining from the plunge of the rotation pole. Tilt or vertical-axis rotation components are larger when the rotation pole is shallower or more steeply plunging, respectively. The resulting tilt and vertical-axis components magnitude were used in this study to choose the preferred net tectonic rotation solutions, complying with the criteria presented in the method section (Table 3).

5. $^{40}\text{Ar}/^{39}\text{Ar}$ Ages

Five samples (BM08SG2, BM000513-06, BM25BT3, BM981107-03, BM010422-07) were crushed to 100–300 μm grain size and subsequently leached with HNO_3 (1 mol/L) for one hour to remove clays and other altered minerals. All samples were finally washed in ultrasonic pure water and acetone. The samples were wrapped in aluminum foil with K_2SO_4 , CaF_2 , and flux monitors of JG-1 biotite. The samples were irradiated for 24 h in the Japan Material Testing Reactor (JMTR), Tohoku University. During the irradiation, samples were shielded by Cd foil in order to reduce neutron-induced ^{40}Ar from ^{40}K . The argon extraction and isotopic analyses were carried out at the Radioisotope Center of the University of Tokyo. The analytical methods are the same as those by Ebisawa et al. (2004). During incremental heating, the gases were extracted in 8 to 11 steps between 500°C and 1,500°C. Note that the sample BM08SG2 was conducted only by six steps (Table 4).

Each result of $^{40}\text{Ar}/^{39}\text{Ar}$ datings provides plateau ages except for the sample BM08SG2 conducted by six steps. The samples of BM000513-06, BM25BT3, BM981107-03, and BM010422-07, yield the plateau ages of 49.9 ± 4.6 Ma [MSWD = 0.37], 41.8 ± 1.1 Ma [MSWD = 1.9], 35.01 ± 0.63 Ma [MSWD = 1.8], and 16.3 ± 1.1 Ma [MSWD = 0.20], respectively. Although the sample of BM08SG2 does not show a plateau age, the weighted average, 53.7 ± 1.2 Ma, during the two steps could be accepted as a result because of their concordant ages with the ^{39}Ar -released more than 84% (Table 4 and Figure 11). Detailed data are available in Table S2.

6. Discussion

6.1. Paleogeographic Constraints

Rocks in accretionary complexes and dismembered ophiolites may have undergone complex tectonic disruptions and vertical axis rotations that prevent to restore due to the lack of continuity of the outcrops.

However, if the magnetizations are primary (i.e., acquired at the time of the rock formation), rocks having a palaeohorizontal position still inform about the palaeolatitude they formed.

The dismembered character and scarcity of outcrops in the MOM hindered the possibility of outcrop scale field test (e.g., fold tests, tilt tests, reversal tests). The inclination of both Cretaceous sites (Site IV and V) fits well only after tilt correction, which indicates a pre-tilting origin for the magnetization of those sites (Table 2). Our pillow basalts and sheeted dolerite dike samples show Fisher precision parameter values (in directions and poles, k & K respectively) below 50; their VGP distributions are rounded (Figure 7) (Table 2); and all pass the Deenen et al. (2011) criteria. All these facts support a primary origin for the magnetization and an adequate average of paleosecular variation. The Site II basalts would be an exception (Figure 8). They show a visibly elongated VGP, although it passes the Deenen criteria. Pillow basalts were < 7 (between

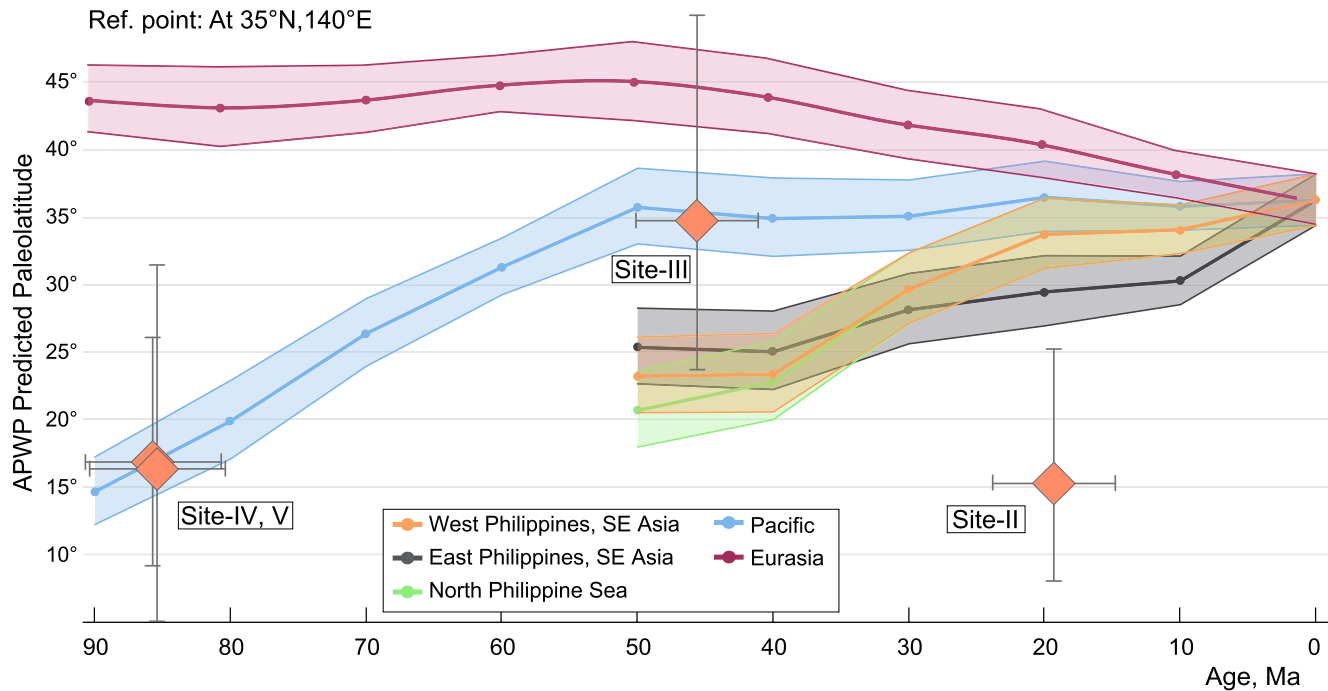


Figure 10. Predicted paleolatitude paths for a reference point (35°N, 150°E) on the Mineoka ophiolite using the Global Apparent Polar Wander Path of Torsvik et al. (2012), in the case that the reference point was attached to the Eurasia, Pacific and Philippine Sea plates, respectively. Dots with uncertainty show the paleomagnetic data by this study for the Mineoka Ophiolite Mélange.

2 and 4) and the result was a deficient average of the PSV resulting in a non-usable result for paleomagnetic directions (Table 2). Sheeted dolerite dikes show two groups that correspond with the different fault bounded blocks sampled. Net tectonic rotation analyses for both blocks show the same pair of directions, which supports a pre-deformation magnetization.

The paleolatitudes obtained from paleomagnetic inclinations in pillow basalts provide the first constraint to evaluate the Mineoka ophiolite motion history and plate origin since the Late Cretaceous. Results from the Site IV and Site V (~85 Ma) show a paleolatitude of N ~16° (Inc. = 30° ± 13°) after tilt correction (Figure 10). Pillow basalts from the Site III are yielded a paleolatitude of N ~34° (Inc. = 54° ± 14°) at ~50 Ma. Those results suggest an 18° paleolatitude shift between 85 Ma to 50 Ma. We interpret that the oceanic crustal rocks in the MOM rocks magnetized in the northern hemisphere due to 4 reasons: (1) The Eocene paleolatitude is the only possible being the northern hemisphere. Otherwise, it would mean Mineoka rocks moved first at least 18° to the south from 85 Ma to 50 Ma (assuming a southern latitude for the Cretaceous pillows) only to flip its motion and move ~70° to the north (~8,000 km) from 50 Ma to present-day; (2) a Cretaceous paleolatitude of 16° to the south would imply ~50° of northwards movement between 85 and 50 Ma. This would require ~5,500 km of northwards convergence at an average speed of 16 cm/yr. So far has not been identified such quick movement in the system, nor a ~E-W slab of that size in the tomography; (3)

Table 3
Results of the Net Tectonic Rotation Analysis Displaying the Two Solutions Obtained at the Site I, Using Normal (N) Polarity Reference Direction

In situ orientation	Ref.dir.	Solution 1						Solution 2					
		Rotation Axis		Rotation		Initial Dike		Rotation Axis		Rotation		Initial Dike	
		Azimuth	Plunge	Magnitude	Sense	Strike	Dip	Azimuth	Plunge	Magnitude	Sense	Strike	Dip
211/25	N	182	9.8	50	CW	122	90	86.6	66.9	67.2	CW	57.9	90
235/10	N	60	32.4	39.4	CW	120.5	90	18.8	32.2	103.8	CW	59.5	90

Solution 2 is preferred.

Table 4
Ar–Ar Age Dating Results From the Mineoka Ophiolite Mélange

Sample information				Total steps	Plateau age					Inverse isochron					
Sample name	Coordinate		Lithology		N	Ma	$\pm 2\sigma$	^{39}Ar	Steps	MSWD	Age		MSWD	$^{40}\text{Ar}/^{36}\text{Ar}$ intercept	
	Latitude	Longitude		%				n			Ma	$\pm 2\sigma$		Ma	$\pm 2\sigma$
BM000513-06	35.1095	139.8507	aphyric tholeiite	8	49.9	4.6	84	0.37	7	48	12	0.40	315	72	4
BM08SG2	35.1087	140.0228	aphyric tholeiite	6	53.7 ^a	1.2	84	-	2	no isochron					
BM25BT3	35.0909	140.1103	cpx-phyric tholeiite	10	41.8	1.1	71	1.9	3	43	4	21	289.0	14.0	10
BM981107-03	35.0906	139.9765	andesite, seriate	11	35	0.6	43	1.8	4	34.7	1.5	3.0	296	3.0	6
BM010422-07	35.1321	139.9341	alkali-basalt	10	16.3	1.1	46	0.20	3	13.9	30	25	318	24	10

^aNo plateau, weighted mean of two fractions.

Cretaceous pillow basalts show downward inclination, and expected in the northern hemisphere during the Cretaceous superchron. (4) Considering a northern hemisphere for all paleolatitudes, they are consistent with the GAPWaP (Torsvik et al., 2012) rotated to the Pacific Plate following Paleomagnetism.org (Koymans et al., 2016) (Figure 10). Our results suggest that the oceanic crustal rocks in the MOM Cretaceous and Eocene rocks moved following the Pacific plate motion. In contrast, none of the Cretaceous to Eocene ophiolitic rocks in the Boso Peninsula could form part of the Philippine Sea Plate, whose paleolatitude at its formation time (~60 Ma) was equatorial (Figure 10). The Miocene alkaline basalt (Site II) exhibits a low paleolatitude of ~16°, inconsistent with both the Pacific Plate and the Philippine Sea Plate at 16 Ma (Figure 10). In addition, the most recent emplacement of Mineoka rocks (19 ± 0.9 Ma) is very close to the time of eruption of the Site II samples (e.g., Mori et al., 2011). The Site II sample results are perhaps the result of a poor average of the PSV leading to a biased shallow inclination. Another possibility is that perhaps these pillow basalts formed with a strong primary tilt following a steep slope of a volcano, which we could not retrieve nor correct.

Sheeted dike complexes in ophiolites form as vertical multiple intrusions subparallel to a spreading ridge that forms them (e.g., MacLeod & Rothery, 1992; Pozzi et al., 1984). During the obduction and emplacement of ophiolites, the effect of regional and local deformation changes the original orientation of the dikes hindering the determination of their initial orientation. Back-tilting dikes to evaluate paleolatitudes usually does not work since a paleohorizontal control is typically not available. Back-tilting sheeted dikes to the vertical may introduce spurious rotations that affect both declination and inclination due to the infinite vertical options around a horizontal axis. The net tectonic rotation analysis on ophiolitic sheeted dikes has been a successful approach to reconstruct the original orientation of dikes in the absence of local paleohorizontal controls (e.g., Morris et al., 1998; Morris & Anderson, 2002; Morris & Maffione, 2016). The net tectonic rotation analyses on the sheeted dikes provided two potential paleo-spreading directions for the Mineoka mid-oceanic ridge. The first solution (Table 3) indicates a minor clockwise rotation but an important tilt of the outcrop. In contrast, the second solution implies a larger clockwise rotation but moderate tilts (Table 3). The Boso Peninsula rotated ~30° clockwise first during the opening of the Japan Sea (e.g., Otofujii & Matsuda, 1983), and later about 50° clockwise after the Izu arc collision forming the Kanto syntaxis (e.g., Hoshi et al., 2013). The pillow basalts' tilt around the sheeted dikes is not steep, which suggests a moderate tilting of the sheeted dikes. The second solution is in agreement with the local structure and it is the one we prefer. This solution indicates an original orientation of the ridge of about ENE 60°.

6.2. Eruption Time and Tectonic Setting

The age spectrum of sample BM010422-07 shows excess argon (^{40}Ar) or partial loss of minor amounts of radiogenic argon component in the first step. This sample yields a spectrum that shows high apparent ages in the initial step (~30 Ma), and the last contiguous steps forming an age plateau. Other samples exhibited a distinct increase or remained stable in dates across an age spectrum from low-temperature to high-temperature extraction steps and show a well-developed plateau spanning more than 50% of the gas released

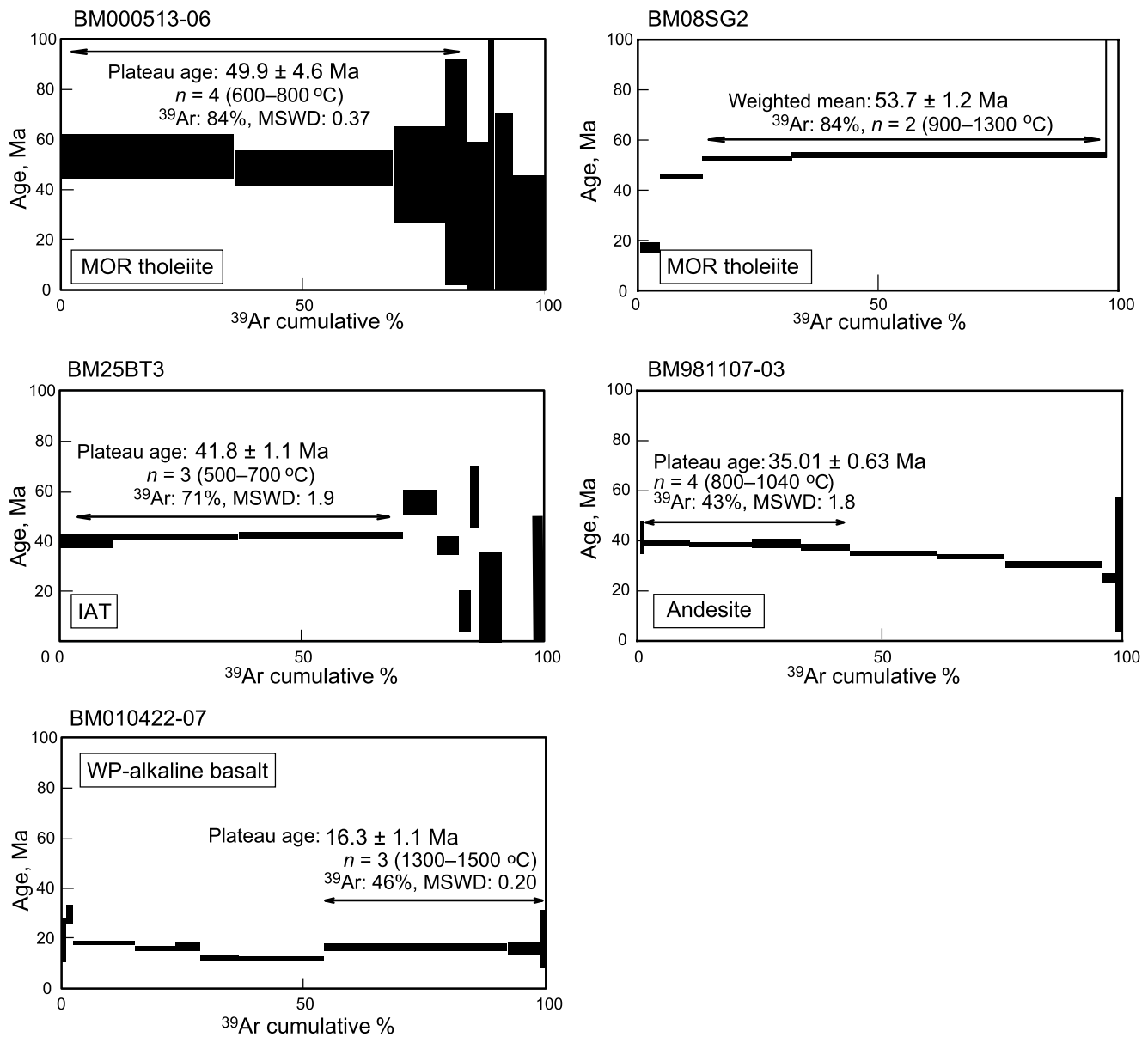


Figure 11. Ar–Ar plateau ages of basaltic and andesitic rocks from Mineoka ophiolite.

and including 3–10 heating steps (Figure 11). These ages are likely to represent the original cooling ages of the volcanic rocks from the Mineoka ophiolite. ⁴⁰Ar/³⁹Ar plateau ages from MORB-like tholeiites yielded 53.7 ± 1.2 Ma and 49.9 ± 4.6 Ma. IAT and andesite are exhibited 41.8 ± 1.1 Ma and 35.1 ± 0.63 Ma. All ages are in agreement with previously reported ages (Hirano et al., 2003). In contrast, alkaline basalt erupted at about 16 ± 1.1 Ma, closer to the timing of the Japan Sea opening.

Supra-subduction ophiolites record subduction initiation, subsequent slab roll-back and extension, and back-arc spreading and leading to the generation of basalt with a MORB-like composition in the former arcs and/or back-arc basins (e.g., Dilek & Furnes, 2011; Shervais et al., 2011). During the back-arc spreading, the basaltic magma is significantly influenced by slab-fluid-induced partial melting of the metasomatized mantle wedge, and various magma mixing (e.g., Dilek & Furnes, 2011). Therefore, their chemistry shows a wide range in composition: N-MORB, IAT, BABB (e.g., Pearce, 2003, 2008). Cretaceous basalts in the MOM show a N-MORB and IAT affinities (Figures 4a–4d). Modern discrimination schemes by Vermeesch (2006a, 2006b) also suggest a N-MORB and IAB geochemical characteristic (Figures 4e and 4f).

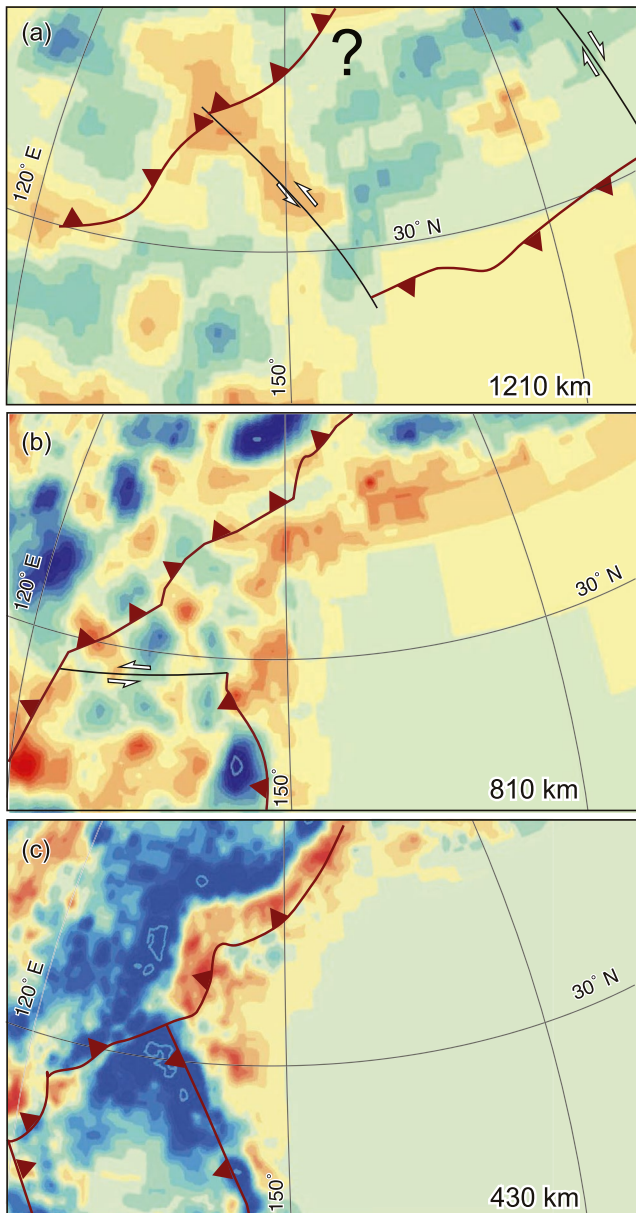


Figure 12. Horizontal depth slices of the present-day mantle tomography images from Atlas of the Underworld (van der Meer et al., 2018), through the UU-P07 Utrecht model (Amaru, 2007). (a) Depths of 1,210 km, and approximately corresponds to Figure 14a; (b) 810 km, to Figure 14b, and (c) 430 km, to Figure 14d of our reconstruction, respectively. Reconstructed positions of the subduction of Pacific, Philippine Sea, and East Asian Sea plates. Question mark reflects the tentative location of the subduction below the north East Asian (Sikhote-Alin) margin.

The presence of plagioclase-bearing peridotites suggest a back-arc setting (e.g., Kimura et al., 2020; Ozawa et al., 2015). In general, the plagioclase peridotites are uncommon among the global abyssal peridotite suites, and have been reported from slow-spreading ridges (e.g., Dick, 1989; Warren, 2016). They have resulted from refertilization of residual peridotite with melt-mantle interaction, as a product of the reaction between peridotite and a melt flow in the lithospheric mantle as shown on some plagioclase peridotites from the Parece Vela back-arc spreading of the Philippine Sea (Ohara et al., 2003). Mineralogical and geochemical features of the Cretaceous basalts in the MOM support an evolution from subduction initiation to a slow spreading back-arc.

Eocene pillow basalts (53–49 Ma) together with 49 Ma dolerite sheeted dikes (Hirano et al., 2003) give evidence that the basaltic magma was extruded in an oceanic spreading ridge. Moreover, their geochemical features (Figure 4) are comparable with the Cretaceous basalts that might have formed in a back-arc spreading. The ~35 Ma gabbros contain some orthopyroxene and show strong island arc affinity (Figure 4). The oceanic arc setting is also supported by the coeval occurrence of granitic rocks (Figure 3). In the MOM, mafic and felsic igneous rocks with typical island arc signature are younger than 41 Ma and older than ~20 Ma, suggesting that the Mineoka was the overriding plate in a convergent margin at least during this time span.

The MOM underwent the tectonic disruptions and hydrothermal alteration before ~15 Ma, because the MOM was overlain by 5–15 Ma undeformed tuffaceous andesites (Ogawa & Takahashi, 2004). Therefore, ocean crust rocks of the MOM including Cretaceous basalts, Eocene arc volcanics, and Miocene alkaline basalts were completely accreted and emplaced before ~15 Ma. As shown by the presence of chlorite, albite, and pumpellyite, these ocean crust rocks underwent a hydrothermal alteration and low-grade metamorphism, perhaps during the accretion. The fault-bounded ~16 Ma alkaline basalts (Figure 2) show very different geochemical features (Figure 4). If the low found paleolatitude was correct, they should have been quite far traveled. However, this hypothesis is not consistent with our present-day knowledge of the area and the regional tectonics. If those volcanic rocks were emplaced tectonically over Japan, they did it shortly after their eruption in a post-spreading setting, concurrent with the Kinan Seamount of the Shikoku Basin (Sato et al., 2002). Nevertheless, those rocks may have erupted directly over Japan.

6.3. Tectonic Model

We propose a preliminary plate reconstruction model in four-time steps as a first attempt to explain the potential plate kinematics of the oceanic crustal rocks of MOM and emplacement into Japan. Our reconstruction is grounded on the previous work by Domeier et al. (2017) and Vaes et al. (2019) for the northern Pacific Plate, and Wu et al. (2016) for the Philippine Sea and East Asian Sea Plates.

We produced a kinematic reconstruction based on the paleomagnetic, geochronological, and geochemical signature of ocean crust rocks of the MOM and tested it against the seismic tomography (Figures 12 and 13). Our tectonic model contains some extinct subduction zones, which were compared with the mantle tomography images from Atlas of the Underworld (van der Meer et al., 2018) of the upper and lower mantle (cf. Domeier et al., 2017; Vaes et al., 2019).

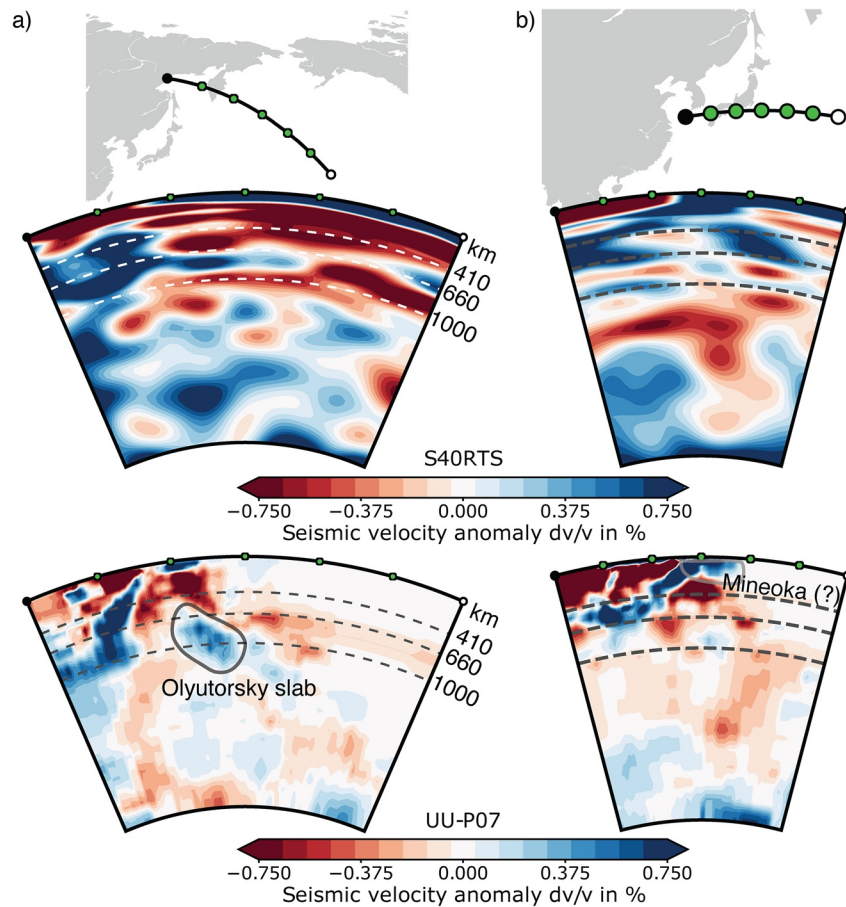


Figure 13. Vertical tomographic cross sections through the (a) East Asia to the Kamchatka; (b) Korea to the Bonin trench. S40RTS is the S-wave model of Ritsema et al., 2011 and UU-P07 is the P-wave model from Utrecht University (Amaru, 2007). The tomographic sections were obtained with SubMachine (Hosseini et al., 2018).

Paleomagnetic poles show that the 85–80 Ma pillow basalts were formed at the paleolatitude of $N \sim 16^\circ$, which is consistent with the paleolatitude of newly formed oceanic crust in the NW Pacific Plate at that time (Figure 14a; Torsvik et al., 2012). We located the eruption of these pillow basalts in the back-arc spreading of the intra-oceanic Nemuro–Olyutorsky arc (Figures 14a and 15a), whose inception and arc development occurred about the same time and same paleolatitude (e.g., Vaes et al., 2019 and references therein). We have fitted the subduction responsible for the formation of this arc with a low-velocity anomaly in the seismic tomography that extends from NW to SE (Figure 13a; Amaru, 2007; Ritsema et al., 2011; van der Meer et al., 2018). We think the shape and extension of such anomaly is possibly controlled by relatively quick roll-back of the slab.

53–49 Ma sheeted dikes and associated pillow basalts, show that the Nemuro–Olyutorsky back-arc ocean was an active divergent margin at least until the Eocene, in a back-arc setting. Paleolatitude extracted from the Eocene pillows indicates that at that time, before the Pacific Plate reorganization (e.g., Domeier et al., 2017) the arc reached $\sim N 34^\circ$, approximately the present-day latitude (Figures 14b and 15b). Net tectonic rotation analyses suggest a paleo-spreading direction of the ridge of 60° at this time. We interpret the obtained paleo-spreading direction as the general ridge orientation. Back-arc ridges are generally sub-parallel to the associated subduction zones, and therefore we tentatively reconstructed the arc and trench with that orientation during the Eocene (Figures 12 and 14a). In our reconstruction, the final collision of the Nemuro–Olyutorsky arc with Japan would trigger a subduction jump and with a flip in its polarity. Subduction possibly initiated parallel to the ridge following, perhaps, an oceanic detachment which is common in slow-spreading systems (see Maffione et al., 2015). After some time of this new subduction scenario, the Mineoka ridge subducted possibly forming a slab window, which in turn facilitated local asthenospheric

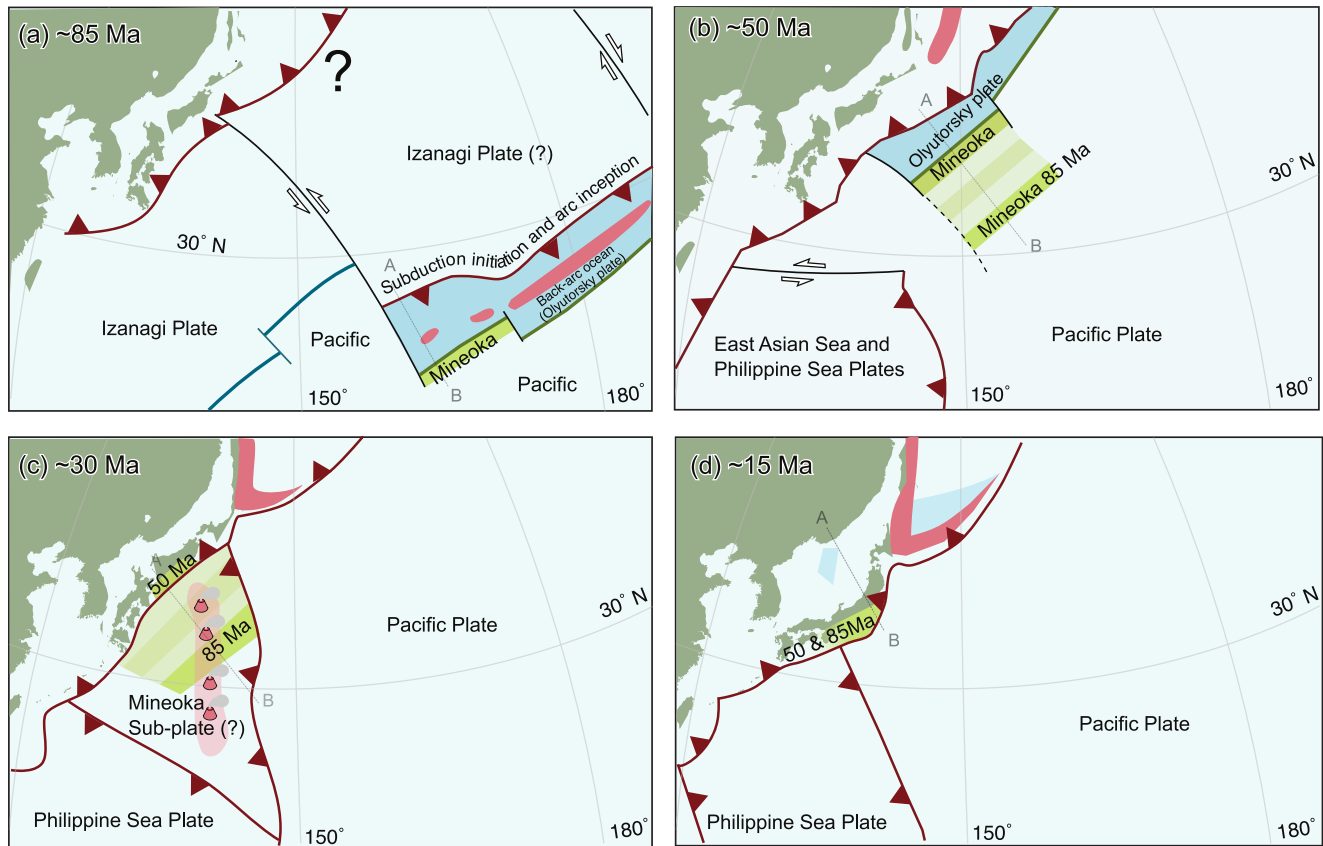


Figure 14. Snapshots of the proposed plate-kinematic reconstruction of the Mineoka ophiolite at NW Pacific region at ca. (a) ~85 Ma, (b) ~50 Ma, (c) ~30 Ma, and (d) ~15 Ma. The red lines represent the reconstructed location of the subduction and triangles are subducting directions. Green lines indicate the Olyutorsky–Pacific plate boundary and its putative isochron, which has originated as a back-arc after the subduction initiation at ~85 Ma. The blue line marks the mid-ocean ridge between Izanagi and Pacific plates. Pink polygons show Nemuro–Olyutorsky arc, light blue polygons outline newly formed oceanic basins, and solid blue polygon marks Olyutorsky plate. The reconstruction follows the mantle reference frame of Doubrovine et al. (2012).

upwelling. The mysterious enhanced thermal gradient formed in the Shimanto Belt during the Late Eocene (Hara & Kimura, 2008; Hasebe & Tagami, 2001) further supports the subduction of ridge during this time. The Mineoka back-arc ridge would have been responsible for such thermal event.

The continuous northward movement accompanied by clockwise rotations of the Philippine Sea Plate (Wu et al., 2016) left a somewhat isolated piece of the Pacific Plate subducting below Japan, a relic of the Mineoka back-arc (Figure 14b). This oceanic crustal piece got trapped in an unstable situation between the E–W motion of the Pacific Plate and the N–S of the Philippine Sea Plate. Under these circumstances, a new subduction zone was initiated within the Pacific Plate following the trend of the Mariana trench and leaving a small triangular sub-plate (so-called Mineoka Plate in Hirano et al., 2003, Figure 14c). Surrounded by convergent boundaries, the fate of the Mineoka sub-plate was a quick consumption below Japan to finally form the Boso triple junction (Figure 1). Subduction below the Mineoka sub-plate (Figures 14c and 15c) can explain the occurrence of 41–20 Ma plutonic rocks and volcanism at this time. A low-velocity anomaly in the shallow depth of seismic tomography possibly indicates the duplication of the Pacific subduction during the formation of the Mineoka sub-plate (Figure 13b). Although similar to the putative Heike Plate of SW Japan (Yamaji & Yoshida, 1998), the Mineoka sub-plate life was longer (since ~85 Ma) and surrounded by convergent boundaries between ~41 and ~20 Ma. The final consumption of the Mineoka sub-plate coincides with the opening of the Japan Sea, when the SW Japan together with the accreted remnants of Mineoka sub-plate rotated clockwise, whereas NE Japan did it counterclockwise (Figures 14d and 15d).

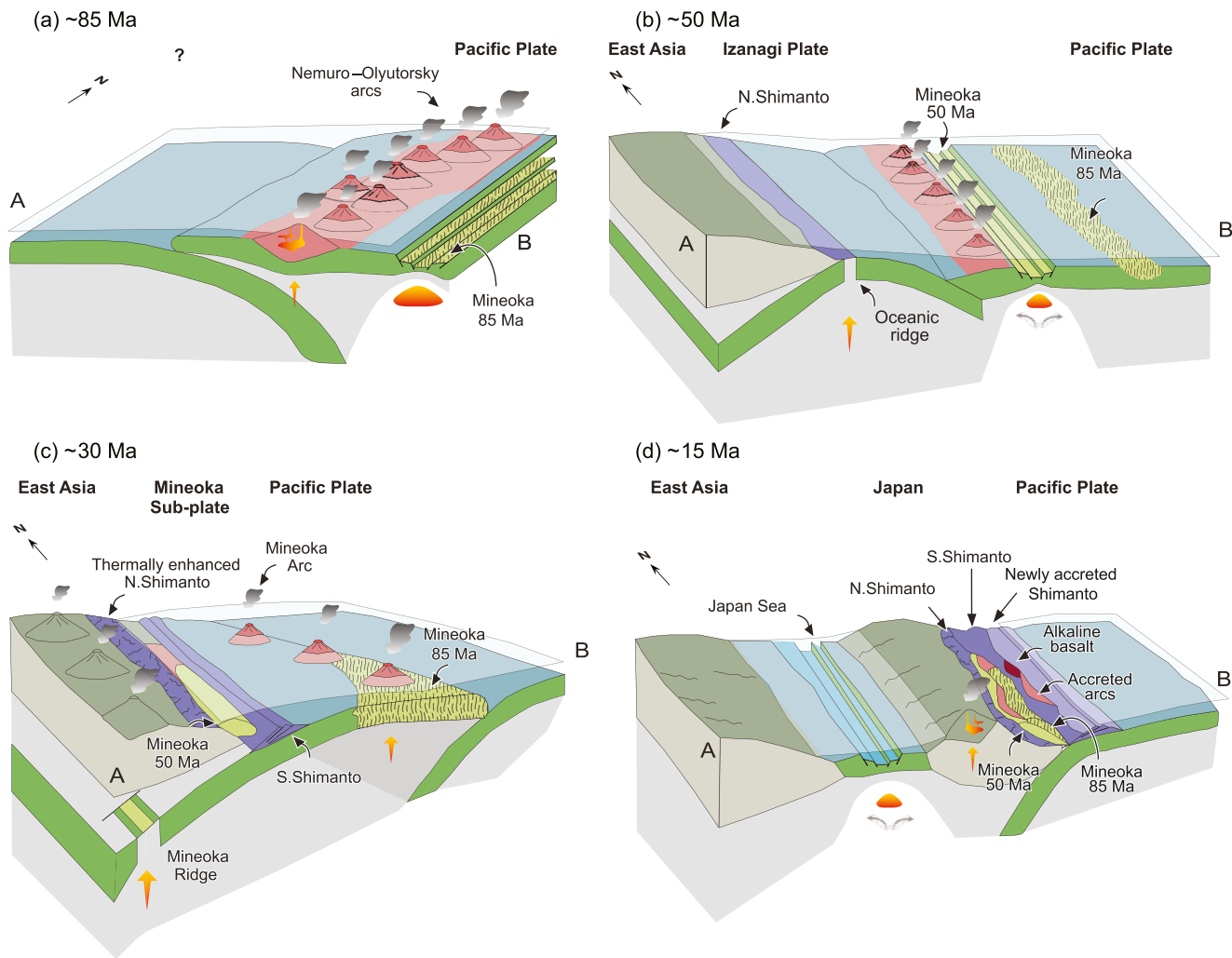


Figure 15. Schematic cross-sections of the proposed plate-kinematic reconstruction of the Mineoka Ophiolite Mélangé at NW Pacific region. Locations are shown in Figure 14. (a) ~85 Ma, the birth of the Mineoka ophiolite in the back-arc spreading ridge of Nemuro–Olyutorsky arcs (b) ~50 Ma, continuously forming Mineoka spreading ridge and demise of the Izanagi Plate under the East Asia (c) ~30 Ma, ridge subduction of the Mineoka ridge thermally enhanced the northern Shimanto Belt and the Pacific Plate is subducting under the Mineoka (d) ~15 Ma, Japan Sea opening and fragments from the Mineoka, together with the Shimanto Belt accreted to Japan.

7. Conclusion

Paleomagnetic analyses in the Mineoka ophiolite showed that the Late Cretaceous pillow basalts extruded at a latitude of $N \sim 16^\circ$ (Inc. = $30^\circ \pm 13^\circ$). The Middle Eocene pillow basalts erupted at $N \sim 34^\circ$ (Inc. = $54^\circ \pm 14^\circ$). The net tectonic rotation analyses on Eocene sheeted dikes from the Benten Island revealed a paleospreading direction of the mid-ocean ridge with a strike of $ENE 60^\circ$. Basalts and andesites are yielded Ar–Ar plateau ages of 49.9 ± 4.6 Ma, 41.8 ± 1.1 Ma, 35.01 ± 0.63 Ma, and 16.3 ± 1.1 Ma and confirmed the previous ages.

Based on our new data, combining together with existing geological, geochemical, and geochronological evidences, we propose a reconstruction of the following steps of tectonic events:

- (1) The Mineoka ophiolite formed as a back-arc spreading ridge of intra-oceanic Nemuro–Olyutorsky arcs during the Late Cretaceous at a paleolatitude of $N \sim 16^\circ$ in the NW Pacific.
- (2) This divergent margin was active until ~49 Ma and spread out to the north at a paleolatitude of $N \sim 34^\circ$, consistent with the Pacific Plate motion. The oceanic spreading ridge direction was $ENE 60^\circ$ during the Eocene.

- (3) A small triangular Mineoka sub-plate left in the gap between the northward moving Philippine Sea Plate with clockwise rotations and the Pacific Plate subducting below Japan. A new subduction zone was initiated within the Pacific Plate under the Mineoka forming 41–20 Ma arc magmatism.
- (4) Surrounding by several active subductions, the newly formed Mineoka sub-plate quickly demised. The final consumption of the Mineoka sub-plate occurred with the opening of the Japan Sea.

Data Availability Statement

All paleomagnetic datasets are available in the online portal paleomagnetism.org. PID: 65ae7d9e-750f72a8279ecc8ae4cb224b1c021975ac1b42c26f7ad52efdb9c75a (<https://paleomagnetism.org/publication/index.html?65ae7d9e750f72a8279ecc8ae4cb224b1c021975ac1b42c26f7ad52efdb9c75a>). Ar–Ar geochronology results have been archived in the EarthChem Library (<https://doi.org/10.26022/IEDA/111767>).

References

- Allerton, S., & Vine, F. J. (1987). Spreading structure of the Troodos ophiolite, Cyprus: Some paleomagnetic constraints. *Geologica*, 15(7), 593–597. [https://doi.org/10.1130/0091-7613\(1987\)15<593:SSOTTO>2.0.CO;2](https://doi.org/10.1130/0091-7613(1987)15<593:SSOTTO>2.0.CO;2)
- Amano, K. (1991). Multiple collision tectonics of the South Fossa Magna in central Japan. *Modern Geology*, 15(4), 315–329.
- Amaru, M. L. (2007). *Global Travel Time Tomography with 3-D Reference Models* (Vol. 274). Utrecht University.
- Aoki, K., Iizuka, T., Hirata, T., Maruyama, S., & Terabayashi, M. (2007). Tectonic boundary between the Sanbagawa belt and the Shimanto belt in central Shikoku, Japan. *The Journal of the Geological Society of Japan*, 113(5), 171–183. <https://doi.org/10.5575/geosoc.113.171>
- Aoki, K., Maruyama, S., Isozaki, Y., Otoh, S., & Yanai, S. (2011). Recognition of the Shimanto HP metamorphic belt within the traditional Sanbagawa HP metamorphic belt: New perspectives of the Cretaceous–Paleogene tectonics in Japan. *Journal of Asian Earth Sciences*, 42(3), 355–369. <https://doi.org/10.1016/j.jseas.2011.05.001>
- Apel, E. V., Bürgmann, R., Steblov, G., Vasilenko, N., King, R., & Prytkov, A. (2006). Independent active microplate tectonics of northeast Asia from GPS velocities and block modeling. *Geophysical Research Letters*, 33(11). <https://doi.org/10.1029/2006gl026077>
- Arai, S. (1991). The Circum-Izu Massif peridotite, central Japan, as back-arc mantle fragments of the Izu-Bonin arc system. In *Ophiolite genesis and evolution of the oceanic lithosphere* (pp. 801–816). Springer. https://doi.org/10.1007/978-94-011-3358-6_40
- Arai, S. (1994). Characterization of spinel peridotites by olivine-spinel compositional relationships: Review and interpretation. *Chemical Geology*, 113(3–4), 191–204. [https://doi.org/10.1016/0009-2541\(94\)90066-3](https://doi.org/10.1016/0009-2541(94)90066-3)
- Arai, S. (2018). Analysis of detritus from mantle-derived rocks. *The Journal of the Geological Society of Japan*, 124(3), 153–169. <https://doi.org/10.5575/geosoc.2017.0068>
- Arai, S., & Ishida, T. (1987). Petrological characteristics of serpentinites in the Kobotoke Group, the Sasago area, Yamanashi Prefecture. A comparison with other Circum-Izu Massif serpentinites. *Journal of Japan Association Mineralogy Petroleum Economy Geology*, 82(9), 336–344. <https://doi.org/10.2465/ganko1941.82.336>
- Arai, S., & Uchida, T. (1978). Highly magnesian dunite from the mineoka belt, central Japan. *Journal of Japan Association Mineralogy Petroleum Economy Geology*, 73(6), 176–179. <https://doi.org/10.2465/ganko1941.73.176>
- Argus, D. F., Gordon, R. G., & DeMets, C. (2011). Geologically current motion of 56 plates relative to the no-net-rotation reference frame. *Geochemistry, Geophysics, Geosystems*, 12(11). <https://doi.org/10.1029/2011GC003751>
- Asada, M., Deschamps, A., Fujiwara, T., & Nakamura, Y. (2007). Submarine lava flow emplacement and faulting in the axial valley of two morphologically distinct spreading segments of the Mariana back-arc basin from Wadatsumi side-scan sonar images. *Geochemistry, Geophysics, Geosystems*, 8(4). <https://doi.org/10.1029/2006GC001418>
- Boschman, L. M., & van Hinsbergen, D. J. J. (2016). On the enigmatic birth of the Pacific Plate within the Panthalassa Ocean. *Science Advances*, 2(7), e1600022. <https://doi.org/10.1126/sciadv.1600022>
- Deenen, M. H. L., Langereis, C. G., van Hinsbergen, D. J. J., & Biggin, A. J. (2011). Geomagnetic secular variation and the statistics of paleomagnetic directions. *Geophysical Journal International*, 186(2), 509–520. <https://doi.org/10.1111/j.1365-246X.2011.05050.x>
- DeMets, C., Gordon, R. G., & Argus, D. F. (2010). Geologically current plate motions. *Geophysical Journal International*, 181(1), 1–80. <https://doi.org/10.1111/j.1365-246X.2009.04491.x>
- Deschamps, A., Fujiwara, T., Asada, M., Montési, L., & Gente, P. (2005). Faulting and volcanism in the axial valley of the slow-spreading center of the Mariana back arc basin from Wadatsumi side-scan sonar images. *Geochemistry, Geophysics, Geosystems*, 6(5), a–n. <https://doi.org/10.1029/2004GC000881>
- Deschamps, A., & Lallemand, S. (2002). The West Philippine Basin: An Eocene to early Oligocene back arc basin opened between two opposed subduction zones. *Journal of Geophysical Research*, 107(B12), 1–1. EPM-1. <https://doi.org/10.1029/2001JB001706>
- Dick, H. J. B. (1989). Abyssal peridotites, very slow spreading ridges and ocean ridge magmatism. *Geological Society, London, Special Publications*, 42(1), 71–105. <https://doi.org/10.1144/gsl.sp.1989.042.01.06>
- Dilek, Y. (2003). *Ophiolite concept and its evolution* (pp. 1–16). Special Papers-Geological Society of America.
- Dilek, Y., & Furnes, H. (2011). Ophiolite genesis and global tectonics: Geochemical and tectonic fingerprinting of ancient oceanic lithosphere. *Geological Society of America Bulletin*, 123(3–4), 387–411. <https://doi.org/10.1130/B30446.1>
- Domeier, M., Shephard, G. E., Jakob, J., Gaina, C., Doubrovine, P. V., & Torsvik, T. H. (2017). Intraoceanic subduction spanned the Pacific in the Late Cretaceous–Paleocene. *Science Advances*, 3(11), eaao2303. <https://doi.org/10.1126/sciadv.aao2303>
- Doubrovine, P. V., Steinberger, B., & Torsvik, T. H. (2012). Absolute plate motions in a reference frame defined by moving hot spots in the Pacific, Atlantic, and Indian oceans. *Journal of Geophysical Research*, 117, L17203. <https://doi.org/10.1029/2011JB009072>
- Ebisawa, N., Sumino, H., Okazaki, R., Takigami, Y., Hirano, N., Nagao, K., & Kaneoka, I. (2004). Construction of I-Xe and 40Ar–39Ar dating system using a modified VG3600 Mass Spectrometer and the first I-Xe data obtained in Japan. *Journal of the Mass Spectrometry Society of Japan*, 52(4), 219–229. <https://doi.org/10.5702/massspec.52.219>
- Engelbreton, D. C. (1985). *Relative Motions between Oceanic and Continental Plates in the Pacific Basin* (Vol. 206). Geological Society of America.

Acknowledgments

This research was supported in part by a Joint Research Grant from CNEAS, Tohoku University to DPG. Ariuntsetseg Ganbat gratefully acknowledges the Japanese Government MEXT Scholarship. Tatsuki Tsujimori gratefully acknowledges MEXT/JSPS KAKENHI support (JP16F16329, 18H01299). Norihiro Nakamura and Naoto Hirano gratefully acknowledge the research grant of Kajima Foundation. The authors also thank Bruno Leite Mendes and Mark Dekkers, Utrecht University for laboratory assistance, and Douwe van der Meer for his very thoughtful comments on the tomography. Constructive reviews by Carmen Gaina and an anonymous reviewer greatly improved this paper.

- Enomoto, H., Ichiyama, Y., & Ito, H. (2018). Early Miocene island arc tholeiite in the Mineoka Belt: Implications for genetic relationship with the Izu-Bonin-Mariana (IBM) arc. *Journal of Mineralogical and Petrological Sciences*, 113(4), 190–197. <https://doi.org/10.2465/jmps.180118>
- Fujioka, K., Tanaka, T., & Aoike, K. (1995). Serpentine Seamount in Izu-Bonin and Mariana Forearcs. Observation by a submersible and its relation to onland serpentinite belt. *Journal of Geography*, 104(3), 473–494. https://doi.org/10.5026/jgeography.104.3_473
- Furnes, H., Dilek, Y., Zhao, G., Safonova, I., & Santosh, M. (2020). Geochemical characterization of ophiolites in the Alpine-Himalayan Orogenic Belt: Magmatically and tectonically diverse evolution of the Mesozoic Neotethyan oceanic crust. *Earth-Science Reviews*, 208, 103258. <https://doi.org/10.1016/j.earscirev.2020.103258>
- Fuston, S., & Wu, J. (2020). Raising the Resurrection plate from an unfolded-slab plate tectonic reconstruction of northwestern North America since early Cenozoic time. *GSA Bulletin*. <https://doi.org/10.1130/B35677.1>
- Grebennikov, A. V., Khanchuk, A. I., Gonevchuk, V. G., & Kovalenko, S. V. (2016). Cretaceous and Paleogene granitoid suites of the Sikhote-Alin area (Far East Russia): Geochemistry and tectonic implications. *Lithos*, 261, 250–261. <https://doi.org/10.1016/j.lithos.2015.12.020>
- Hall, R., Ali, J. R., & Anderson, C. D. (1995a). Cenozoic motion of the Philippine Sea Plate: Paleomagnetic evidence from eastern Indonesia. *Tectonics*, 14, 1117–1132. <https://doi.org/10.1029/95TC01694>
- Hall, R., Ali, J. R., Anderson, C. D., & Baker, S. J. (1995b). Origin and motion history of the Philippine Sea Plate. *Tectonophysics*, 251(1–4), 229–250. [https://doi.org/10.1016/0040-1951\(95\)00038-0](https://doi.org/10.1016/0040-1951(95)00038-0)
- Hall, R., & Spakman, W. (2002). Subducted slabs beneath the eastern Indonesia-Tonga region: Insights from tomography. *Earth and Planetary Science Letters*, 201(2), 321–336. [https://doi.org/10.1016/S0012-821X\(02\)00705-7](https://doi.org/10.1016/S0012-821X(02)00705-7)
- Hara, H., & Kimura, K. (2008). Metamorphic and cooling history of the Shimanto accretionary complex, Kyushu, Southwest Japan: Implications for the timing of out-of-sequence thrusting. *Island Arc*, 17(4), 546–559. <https://doi.org/10.1111/j.1440-1738.2008.00636.x>
- Harada, H., Tsujimori, T., Kunugiza, K., Yamashita, K., Aoki, S., Aoki, K., et al. (2021). The $\delta^{13}\text{C}$ - $\delta^{18}\text{O}$ variations in marble in the Hida Belt, Japan. *Island Arc*, 30, e12389. <https://doi.org/10.1111/iar.12389>
- Hasebe, N., & Tagami, T. (2001). Exhumation of an accretionary prism - results from fission track thermochronology of the Shimanto Belt, southwest Japan. *Tectonophysics*, 331(3), 247–267. [https://doi.org/10.1016/S0040-1951\(00\)00282-1](https://doi.org/10.1016/S0040-1951(00)00282-1)
- Haston, R. B., & Fuller, M. (1991). Paleomagnetic data from the Philippine Sea plate and their tectonic significance. *Journal of Geophysical Research*, 96(B4), 6073–6098. <https://doi.org/10.1029/90JB02700>
- Hickey-Vargas, R. (2005). Basalt and tonalite from the Amami Plateau, northern West Philippine Basin: New Early Cretaceous ages and geochemical results, and their petrologic and tectonic implications. *Island Arc*, 14(4), 653–665. <https://doi.org/10.1111/j.1440-1738.2005.00474.x>
- Hirano, N., Ogawa, Y., Saito, K., Yoshida, T., Sato, H., & Taniguchi, H. (2003). Multi-stage evolution of the Tertiary Mineoka ophiolite, Japan: New geochemical and age constraints. *Geological Society*, 218(1), 279–298. <https://doi.org/10.1144/GSL.SP.2003.218.01.15>
- Hirano, N., & Okuzawa, K. (2002). Occurrence of the sandstone included in the alkali-basalt lava flow from the western Mineoka Belt, Boso Peninsula, Japan, and its tectonic significance. *The Journal of the Geological Society of Japan*, 108(11), 691–700. https://doi.org/10.5575/geosoc.108.11_691
- Hiroi, Y., Harada-Kondo, H., & Ogo, Y. (1992). Cuprian manganian phlogopite in highly oxidized Mineoka siliceous schists from Kamogawa, Boso Peninsula, central Japan. *American Mineralogist*, 77(9–10), 1099–1106.
- Hoshi, H., & Sano, M. (2013). Paleomagnetic constraints on Miocene rotation in the central Japan Arc. *Island Arc*, 22(2), 197–213. <https://doi.org/10.1111/iar.12022>
- Hosseini, K., Matthews, K. J., Sigloch, K., Shephard, G. E., Domeier, M., & Tsekhmistrenko, M. (2018). Submachine: Web-based tools for exploring seismic tomography and other models of earth's deep interior. *Geochemistry, Geophysics, Geosystems*, 19(5), 1464–1483. <https://doi.org/10.1029/2018GC007431>
- Hutchison, C. S. (1989). *Geological Evolution of South-East Asia* (Vol. 13, p. 368). Clarendon Press.
- Ichiyama, Y., Ishiwatari, A., & Koizumi, K. (2008). Petrogenesis of greenstones from the Mino-Tamba belt, SW Japan: Evidence for an accreted Permian oceanic plateau. *Lithos*, 100(1–4), 127–146. <https://doi.org/10.1016/j.lithos.2007.06.014>
- Ichiyama, Y., Ito, H., Hokanishi, N., Tamura, A., & Arai, S. (2017). Plutonic rocks in the Mineoka-Setogawa ophiolitic mélange, central Japan: Fragments of middle to lower crust of the Izu-Bonin-Mariana Arc?. *Lithos*, 282–283, 420–430. <https://doi.org/10.1016/j.lithos.2017.03.021>
- Ichiyama, Y., Ito, H., Tamura, A., & Arai, S. (2020). Magma mixing model for the genesis of middle crust in the Izu-Bonin-Mariana arc: Evidence from plutonic rocks in the Mineoka-Setogawa ophiolitic mélange, central Japan. *International Geology Review*, 62(4), 503–521. <https://doi.org/10.1080/00206814.2019.1621779>
- Ishiwatari, A. (1994). Circum-Pacific Phanerozoic multiple ophiolite belts. In A. Ishiwatari, J. Malpas, J., & H. Ishizuka (Eds.), *Circum-pacific ophiolites* (pp. 7–28).
- Ishiwatari, A., Ozawa, K., Arai, S., Ishimaru, S., Abe, N., & Takeuchi, M. (2016). Ophiolites and ultramafic rocks. In T. Moreno, S. R. Wallis, T. Kojima, & W. Gibbons Eds., *The Geology of Japan* (pp. 223–250). The Geological Society of London. <https://doi.org/10.1144/GOJ.9>
- Ishizuka, O., Taylor, R. N., Ohara, Y., & Yuasa, M. (2013). Upwelling, rifting, and age-progressive magmatism from the Okai-Daito mantle plume. *Geology*, 41(9), 1011–1014. <https://doi.org/10.1130/G34525.1>
- Ishizuka, O., & Yuasa, M. (2007). Age and geochemical characteristics of the igneous rocks recovered the Philippine Sea and Ogasawara Plateau area as a part of basic researches on exploration technologies for deep-sea natural resources. In *Rep on deep sea survey technology for natural resources in Japan* (pp. 255–296). JOGMEC.
- Isozaki, Y. (1996). Anatomy and genesis of a subduction-related orogen: A new view of geotectonic subdivision and evolution of the Japanese Islands. *Island Arc*, 5, 289–320. <https://doi.org/10.1111/j.1440-1738.1996.tb00033.x>
- Isozaki, Y., Aoki, K., Nakama, T., & Yanai, S. (2010). New insight into a subduction-related orogen: A reappraisal of the geotectonic framework and evolution of the Japanese Islands. *Gondwana Research*, 18(1), 82–105. <https://doi.org/10.1016/j.gr.2010.02.015>
- Itaya, T., Tsujimori, T., & Liou, J. G. (2011). Evolution of the Sanbagawa and Shimanto high-pressure belts in SW Japan: Insights from K-Ar (Ar-Ar) geochronology. *Journal of Asian Earth Sciences*, 42(6), 1075–1090. <https://doi.org/10.1016/j.jseaeas.2011.06.012>
- Jahn, B.-m., Valui, G., Kruk, N., Gonevchuk, V., Usuki, M., & Wu, J. T. J. (2015). Emplacement ages, geochemical and Sr-Nd-Hf isotopic characterization of Mesozoic to early Cenozoic granitoids of the Sikhote-Alin Orogenic Belt, Russian Far East: Crustal growth and regional tectonic evolution. *Journal of Asian Earth Sciences*, 111, 872–918. <https://doi.org/10.1016/j.jseaeas.2015.08.012>
- John, T., & Schenk, V. (2003). Partial eclogitization of gabbroic rocks in a late Precambrian subduction zone (Zambia): Prograde metamorphism triggered by fluid infiltration. *Contributions to Mineralogy and Petrology*, 146(2), 174–191. <https://doi.org/10.1007/s00410-003-0492-8>

- Kimura, G., Hashimoto, Y., Yamaguchi, A., Kitamura, Y., & Ujiie, K. (2016). Cretaceous-Neogene accretionary units. In T. Moreno, S. R. Wallis, T. Kojima, & W. Gibbons Eds., *The Geology of Japan* (pp. 125–137). The Geological Society of London. <https://doi.org/10.1144/GOJ.5>
- Kimura, T., Ozawa, K., Kuritani, T., Iizuka, T., & Nakagawa, M. (2020). Thermal state of the upper mantle and the origin of the Cambrian-Ordovician ophiolite pulse: Constraints from ultramafic dikes of the Hayachine-Miyamori ophiolite. *American Mineralogist*, 105, 1778–1801. <https://doi.org/10.2138/am-2020-7160>
- Kirschvink, J. L. (1980). The least-squares line and plane and the analysis of paleomagnetic data. *Geophysical Journal International*, 62(3), 699–718. <https://doi.org/10.1111/j.1365-246x.1980.tb02601.x>
- Koyama, M. (1991). Tectonic evolution of the Philippine Sea Plate based on paleomagnetic results. *Journal of Geography*, 100(4), 628–641. <https://doi.org/10.5026/jgeography.100.628>
- Koymans, M. R., Hinsbergen, D. J. J., Pastor-Galán, D., Vaes, B., & Langereis, C. G. (2020). Toward FAIR Paleomagnetic Data Management Through Paleomagnetism.org 2.0. *Geochemistry, Geophysics, Geosystems*, 21(2), e2019GC008838. <https://doi.org/10.1029/2019GC008838>
- Koymans, M. R., Langereis, C. G., Pastor-Galán, D., & van Hinsbergen, D. J. J. (2016). Paleomagnetism.org: An online multi-platform open source environment for paleomagnetic data analysis. *Computers & Geosciences*, 93, 127–137. <https://doi.org/10.1016/j.cageo.2016.05.007>
- Lallemand, S. (2016). Philippine Sea Plate inception, evolution, and consumption with special emphasis on the early stages of Izu-Bonin-Mariana subduction. *Progress in Earth and Planetary Science*, 3(1), 15. <https://doi.org/10.1186/s40645-016-0085-6>
- Larson, E. E., Reynolds, R. L., Ozima, M., Aoki, Y., Kinoshita, H., Zasshu, S., et al. (1975). Paleomagnetism of miocene volcanic rocks of guam and the curvature of the southern Mariana Island Arc. *The Geological Society of America Bulletin*, 86(3), 346–350. [https://doi.org/10.1130/0016-7606\(1975\)86<346:POMVRO>2.0.CO;2](https://doi.org/10.1130/0016-7606(1975)86<346:POMVRO>2.0.CO;2)
- Levashova, N. M., Shapiro, M. N., Beniamovsky, V. N., & Bazhenov, M. L. (2000). Paleomagnetism and geochronology of the Late Cretaceous-Paleogene island arc complex of the Kronotsky Peninsula, Kamchatka, Russia: Kinematic implications. *Tectonics*, 19(5), 834–851. <https://doi.org/10.1029/1998TC001087>
- Li, C., van der Hilst, R. D., Engdahl, E. R., & Burdick, S. (2008). A new global model for P-wave speed variations in Earth's mantle. *Geochemistry, Geophysics, Geosystems*, 9, Q05018. <https://doi.org/10.1029/2007GC001806>
- Li, X.-h. (2000). Cretaceous magmatism and lithospheric extension in Southeast China. *Journal of Asian Earth Sciences*, 18(3), 293–305. [https://doi.org/10.1016/S1367-9120\(99\)00060-7](https://doi.org/10.1016/S1367-9120(99)00060-7)
- Li, Z., Qiu, J.-S., & Yang, X.-M. (2014). A review of the geochronology and geochemistry of Late Yanshanian (Cretaceous) plutons along the Fujian coastal area of southeastern China: Implications for magma evolution related to slab break-off and rollback in the Cretaceous. *Earth-Science Reviews*, 128, 232–248. <https://doi.org/10.1016/j.earscirev.2013.09.007>
- Liu, K., Zhang, J., Xiao, W., Wilde, S. A., & Alexandrov, I. (2020). A review of magmatism and deformation history along the NE Asian margin from ca. 95 to 30 Ma: Transition from the Izanagi to Pacific plate subduction in the early Cenozoic. *Earth-Science Reviews*, 209, 103317. <https://doi.org/10.1016/j.earscirev.2020.103317>
- Liu, L., Xu, X., & Xia, Y. (2014). Cretaceous Pacific plate movement beneath SE China: Evidence from episodic volcanism and related intrusions. *Tectonophysics*, 614, 170–184. <https://doi.org/10.1016/j.tecto.2013.12.007>
- Lonsdale, P. (1988). Geography and history of the Louisville hotspot chain in the southwest Pacific. *Journal of Geophysical Research*, 93(B4), 3078–3104. <https://doi.org/10.1029/JB093iB04p03078>
- Louden, K. E. (1977). Paleomagnetism of DSDP sediments, phase shifting of magnetic anomalies, and rotations of the West Philippine Basin. *Journal of Geophysical Research*, 82(20), 2989–3002. <https://doi.org/10.1029/JB082i020p02989>
- MacLeod, C. J., & Rothery, D. A. (1992). Ridge axial segmentation in the Oman ophiolite: Evidence from along-strike variations in the sheeted dyke complex. *Geological Society*, 60(1), 39–63. <https://doi.org/10.1144/GSL.SP.1992.060.01.03>
- Maffione, M., Thieulot, C., Van Hinsbergen, D. J. J., Morris, A., Plümper, O., & Spakman, W. (2015). Dynamics of intraoceanic subduction initiation: 1. Oceanic detachment fault inversion and the formation of supra-subduction zone ophiolites. *Geochemistry, Geophysics, Geosystems*, 16(6), 1753–1770. <https://doi.org/10.1002/2015GC005746>
- Maffione, M., & van Hinsbergen, D. J. J. (2018). Reconstructing plate boundaries in the Jurassic Neo-Tethys from the East and West Vardar Ophiolites (Greece and Serbia). *Tectonics*, 37(3), 858–887. <https://doi.org/10.1002/2017TC004790>
- Maruyama, S., Isozaki, Y., Kimura, G., & Terabayashi, M. (1997). Paleogeographic maps of the Japanese Islands: Plate tectonic synthesis from 750 Ma to the present. *Island Arc*, 6(1), 121–142. <https://doi.org/10.1111/j.1440-1738.1997.tb00043.x>
- Maruyama, S., & Send, T. (1986). Orogeny and relative plate motions: Example of the Japanese Islands. *Tectonophysics*, 127, 305–329. [https://doi.org/10.1016/0040-1951\(86\)90067-3](https://doi.org/10.1016/0040-1951(86)90067-3)
- Metcalfe, I. (2011). Tectonic framework and Phanerozoic evolution of Sundaland. *Gondwana Research*, 19(1), 3–21. <https://doi.org/10.1016/j.gr.2010.02.016>
- Mohiuddin, M. M., & Ogawa, Y. (1998). Late Paleocene-middle Miocene pelagic sequences in the Boso Peninsula, Japan: New light on northwest Pacific tectonics. *Island Arc*, 7(3), 301–314. <https://doi.org/10.1111/j.1440-1738.1998.00191.x>
- Mori, R., & Ogawa, Y. (2005). Transpressional tectonics of the Mineoka Ophiolite Belt in a trench-trench-trench-type triple junction, Boso Peninsula, Japan. *Island Arc*, 14(4), 571–581. <https://doi.org/10.1111/j.1440-1738.2005.00485.x>
- Mori, R., Ogawa, Y., Hirano, N., Tsunogae, T., Kurosawa, M., & Chiba, T. (2011). Role of plutonic and metamorphic block exhumation in a forearc ophiolite mélange belt: An example from the Mineoka belt, Japan. *Geological Society of America Special Paper*, 480, 95–115.
- Morris, A., & Anderson, M. W. (2002). Paleomagnetic results from the Baër-Bassit ophiolite of northern Syria and their implication for fold tests in sheeted dyke terrains. *Physics and Chemistry of the Earth, Parts A/B/C*, 27(25–31), 1215–1222. [https://doi.org/10.1016/S1547-7065\(02\)00123-7](https://doi.org/10.1016/S1547-7065(02)00123-7)
- Morris, A., Anderson, M. W., & Robertson, A. H. (1998). Multiple tectonic rotations and transform tectonism in an intra-oceanic suture zone, SW Cyprus. *Tectonophysics*, 299(1–3), 229–253. [https://doi.org/10.1016/S0040-1951\(98\)00207-8](https://doi.org/10.1016/S0040-1951(98)00207-8)
- Morris, A., & Maffione, M. (2016). Is the Troodos ophiolite (Cyprus) a complete, transform fault-bounded Neotethyan ridge segment?. *Geology*, 44(3), 199–202. <https://doi.org/10.1130/G37529.1>
- Mullender, T. A. T., Velzen, A. J., & Dekkers, M. J. (1993). Continuous drift correction and separate identification of ferrimagnetic and paramagnetic contributions in thermomagnetic runs. *Geophysical Journal International*, 114(3), 663–672. <https://doi.org/10.1111/j.1365-246X.1993.tb06995.x>
- Müller, R. D., Seton, M., Zahirovic, S., Williams, S. E., Matthews, K. J., Wright, N. M., et al. (2016). Ocean basin evolution and global-scale plate reorganization events since Pangea breakup. *Annual Review of Earth and Planetary Sciences*, 44, 107–138. <https://doi.org/10.1146/annurev-earth-060115-012211>
- Nishizawa, A., Kaneda, K., Katagiri, Y., & Oikawa, M. (2014). Wide-angle refraction experiments in the Daito Ridges region at the north-western end of the Philippine Sea plate. *Earth Planets and Space*, 66(1), 1–16. <https://doi.org/10.1186/1880-5981-66-25>

- Ogawa, Y., Mori, R., Hirano, N., Takahashi, A., Mohiuddin, M. M., Sato, H., & Chiba, T. (2009). Knocker catalog of the Mineoka ophiolite belt, Boso Peninsula, Japan. *Earth Evolution Sciences*, 3, 3–25.
- Ogawa, Y., & Sashida, K. (2005). Lower Cretaceous radiolarian bedded chert from the Mineoka Belt, Boso Peninsula, Japan. *The Journal of the Geological Society of Japan*, 111(10), 624–627. <https://doi.org/10.5575/geosoc.111.624>
- Ogawa, Y., & Takahashi, A. (2004). Seafloor spreading, obduction and triple junction tectonics of the Mineoka Ophiolite, Central Japan. *Tectonophysics*, 392(1–4), 131–141. <https://doi.org/10.1016/j.tecto.2004.08.007>
- Ogawa, Y., & Taniguchi, H. (1987). Ophiolite mélange in the forearc areas and the development of the Mineoka Belt. *Science Reports, Department of Geology, Kyushu University*, 15, 1–23.
- Ogawa, Y., & Taniguchi, H. (1988). Geology and tectonics of the Miura–Boso Peninsulas and the adjacent area. *Modern Geology*, 12, 147–168.
- Ohara, Y., Fujioka, K., Ishii, T., & Yurimoto, H. (2003). Peridotites and gabbros from the Parece Vela backarc basin: Unique tectonic window in an extinct backarc spreading ridge. *Geochemistry, Geophysics, Geosystems*, 4(7). <https://doi.org/10.1029/2002GC000469>
- Otofujii, Y., & Matsuda, T. (1983). Paleomagnetic evidence for the clockwise rotation of Southwest Japan. *Earth and Planetary Science Letters*, 62(3), 349–359. [https://doi.org/10.1016/0012-821X\(83\)90005-5](https://doi.org/10.1016/0012-821X(83)90005-5)
- Ozawa, K., Maekawa, H., Shibata, K., Asahara, Y., & Yoshikawa, M. (2015). Evolution processes of Ordovician-Devonian arc system in the South-Kitakami Massif and its relevance to the Ordovician ophiolite pulse. *Island Arc*, 24, 73–118. <https://doi.org/10.1111/iar.12100>
- Pastor-Galán, D., Spencer, C. J., Furukawa, T., & Tsujimori, T. (2021). Evidence for crustal removal, tectonic erosion and flare-ups from the Japanese evolving forearc sediment provenance. *Earth and Planetary Science Letters*, 564, 116893. <https://doi.org/10.1016/j.epsl.2021.116893>
- Pearce, J. A. (2003). Supra-subduction zone ophiolites: The search for modern analogs. *Geological Society of America*, 373, 269–294.
- Pearce, J. A. (2008). Geochemical fingerprinting of oceanic basalts with applications to ophiolite classification and the search for Archean oceanic crust. *Lithos*, 100(1–4), 14–48. <https://doi.org/10.1016/j.lithos.2007.06.016>
- Pearce, J. A., & Norry, M. J. (1979). Petrogenetic implications of Ti, Zr, Y, and Nb variations in volcanic rocks. *Contributions to Mineralogy and Petrology*, 69(1), 33–47. <https://doi.org/10.1007/bf00375192>
- Pozzi, J. P., Westphal, M., Girardeau, J., Besse, J., Yao Xiu Zhou, X. Y., & Li Sheng Xing, L. S. (1984). Paleomagnetism of the Xigaze ophiolite and flysch (Yarlung Zangbo suture zone, southern Tibet): Latitude and direction of spreading. *Earth and Planetary Science Letters*, 70(2), 383–394. [https://doi.org/10.1016/0012-821X\(84\)90022-0](https://doi.org/10.1016/0012-821X(84)90022-0)
- Raimbourg, H., Famin, V., Palazzin, G., Yamaguchi, A., & Augier, R. (2017). Tertiary evolution of the Shimanto belt (Japan): A large-scale collision in Early Miocene. *Tectonics*, 36(7), 1317–1337. <https://doi.org/10.1002/2017TC004529>
- Ren, J., Tamaki, K., Li, S., & Junxia, Z. (2002). Late Mesozoic and Cenozoic rifting and its dynamic setting in Eastern China and adjacent areas. *Tectonophysics*, 344(3–4), 175–205. [https://doi.org/10.1016/S0040-1951\(01\)00271-2](https://doi.org/10.1016/S0040-1951(01)00271-2)
- Richter, C., & Ali, J. R. (2015). Philippine sea plate motion history: Eocene-Recent record from ODP Site 1201, central West Philippine basin. *Earth and Planetary Science Letters*, 410, 165–173. <https://doi.org/10.1016/j.epsl.2014.11.032>
- Ritsema, J., Deuss, A., Van Heijst, H. J., & Woodhouse, J. H. (2011). S4ORTS: A degree-40 shear-velocity model for the mantle from new Rayleigh wave dispersion, teleseismic traveltime and normal-mode splitting function measurements. *Geophysical Journal International*, 184(3), 1223–1236. <https://doi.org/10.1111/j.1365-246x.2010.04884.x>
- Rodnikov, A. G., Zabarinskaya, L. P., Sergeeva, N. A., & Nisilevich, M. V. (2013). Geodynamic models of deep structure of regions of natural hazards of the Eurasia–Pacific transition zone. *Vestn. Otd. nauk Zemle*, 5. <https://doi.org/10.2205/2013nz000118>
- Sakai, H. (1988). Toi-misaki olistostrome of the Southern Belt of the Shimanto Terrane, South Kyushu: Reconstruction of depositional environments and stratigraphy before the collapse. *The Journal of the Geological Society of Japan*, 94, 733–747. <https://doi.org/10.5575/geosoc.94.733>
- Saper, L., & Liang, Y. (2014). Formation of plagioclase-bearing peridotite and plagioclase-bearing wehrlite and gabbro suite through reactive crystallization: An experimental study. *Contributions to Mineralogy and Petrology*, 167(3), 985. <https://doi.org/10.1007/s00410-014-0985-7>
- Sasaki, T., Yamazaki, T., & Ishizuka, O. (2014). A revised spreading model of the West Philippine Basin. *Earth Planets and Space*, 66(1), 83. <https://doi.org/10.1186/1880-5981-66-83>
- Sato, H., Machida, S., Kanayama, S., Taniguchi, H., & Ishii, T. (2002). Geochemical and isotopic characteristics of the Kinan Seamount Chain in the Shikoku Basin. *Geochemical Journal*, 36(5), 519–526. <https://doi.org/10.2343/geochemj.36.519>
- Sdrolias, M., Roest, W. R., & Müller, R. D. (2004). An expression of Philippine Sea plate rotation: The Parece Vela and Shikoku basins. *Tectonophysics*, 394(1–2), 69–86. <https://doi.org/10.1016/j.tecto.2004.07.061>
- Seno, T., & Maruyama, S. (1984). Paleogeographic reconstruction and origin of the Philippine Sea. *Tectonophysics*, 102(1–4), 53–84. [https://doi.org/10.1016/0040-1951\(84\)90008-8](https://doi.org/10.1016/0040-1951(84)90008-8)
- Seno, T., Sakurai, T., & Stein, S. (1996). Can the Okhotsk plate be discriminated from the North American plate? *Journal of Geophysical Research*, 101(B5), 11305–11315. <https://doi.org/10.1029/96JB00532>
- Seton, M., Flament, N., Whittaker, J., Müller, R. D., Gurnis, M., & Bower, D. J. (2015). Ridge subduction sparked reorganization of the Pacific plate-mantle system 60–50 million years ago. *Geophysical Research Letters*, 42(6), 1732–1740. <https://doi.org/10.1002/2015GL063057>
- Seton, M., Müller, R. D., Zahirovic, S., Gaina, C., Torsvik, T., Shephard, G., et al. (2012). Global continental and ocean basin reconstructions since 200Ma. *Earth-Science Reviews*, 113(3–4), 212–270. <https://doi.org/10.1016/j.earscirev.2012.03.002>
- Shervais, J. W., Choi, S. H., Sharp, W. D., Ross, J., Zoglman-Schuman, M., & Mukasa, S. B. (2011). Serpentinite matrix mélange: Implications of mixed provenance for mélange formation. *Geological Society of America Special Paper*, 480, 1–30.
- Sigloch, K., & Mihalynuk, M. G. (2013). Intra-oceanic subduction shaped the assembly of Cordilleran North America. *Nature*, 496(7443), 50–56. <https://doi.org/10.1038/nature12019>
- Solov'ev, A. V., Garver, J. I., Shapiro, M. N., Brandon, M. T., & Hourigan, J. K. (2011). Eocene arc-continent collision in northern Kamchatka, Russian Far East. *Russian Journal of Earth Sciences*, 12, 1–13.
- Taira, A. (1988). The shimanto belt in Shikoku, Japan: Evolution of Cretaceous to Miocene accretionary prism. *Modern Geology*, 12, 5–46.
- Takahashi, A., Ogawa, Y., Ohta, Y., & Hirano, N. (2003). The nature of faulting and deformation in the Mineoka Ophiolite, NW Pacific Rim. *Geological Society*, 218(1), 299–314. <https://doi.org/10.1144/GSL.SP.2003.218.01.16>
- Takahashi, M., & Saito, K. (1997). Miocene intra-arc bending at an arc-arc collision zone, central Japan. *Island Arc*, 6(2), 168–182. <https://doi.org/10.1111/j.1440-1738.1997.tb00168.x>
- Takahashi, N. (1994). Alkali basalt-clastic sequence in the west end of the Mineoka Belt, Boso Peninsula, Japan. *Journal of Natural History Museum and Institute, Chiba*, 3, 1–18.

- Tatsumi, Y., Kani, T., Ishizuka, H., Maruyama, S., & Nishimura, Y. (2000). Activation of Pacific mantle plumes during the Carboniferous: Evidence from accretionary complexes in southwest Japan. *Geology*, 28(7), 580–582. [https://doi.org/10.1130/0091-7613\(2000\)28<580:AOPMPD>2.0.CO;2](https://doi.org/10.1130/0091-7613(2000)28<580:AOPMPD>2.0.CO;2)
- Tokuyama, H. (1986). Marine geology and subcrustal structure of the Shikoku Basin and the Daito Ridges region in the northern Philippine Sea. *Bulletin of the Ocean Research Institute, University of Tokyo*, 22, 1–169.
- Tokuyama, H. (2007). Tectonic development and reconstruction of Philippine Sea Plate since late Cretaceous. In *Report on deep sea survey technology for natural resources in Japan, JOGMEC* (pp. 430–456).
- Torsvik, T. H., Van der Voo, R., Preeden, U., Mac Niocaill, C., Steinberger, B., Doubrovine, P. V., et al. (2012). Phanerozoic polar wander, paleogeography and dynamics. *Earth-Science Reviews*, 114(3–4), 325–368. <https://doi.org/10.1016/j.earscirev.2012.06.007>
- Tsujimori, T., & Liou, J. G. (2005). Eclogite-facies mineral inclusions in clinozoisite from Paleozoic blueschist, central Chugoku Mountains, southwest Japan: Evidence of regional eclogite-facies metamorphism. *International Geology Review*, 47, 215–232. <https://doi.org/10.2747/0020-6814.47.3.215>
- Vaes, B., Hinsbergen, D. J. J., & Boschman, L. M. (2019). Reconstruction of subduction and back-arc spreading in the NW Pacific and Aleutian Basin: Clues to causes of cretaceous and eocene plate reorganizations. *Tectonics*, 38(4), 1367–1413. <https://doi.org/10.1029/2018TC005164>
- van der Meer, D. G., Van Hinsbergen, D. J. J., & Spakman, W. (2018). Atlas of the underworld: Slab remnants in the mantle, their sinking history, and a new outlook on lower mantle viscosity. *Tectonophysics*, 723, 309–448. <https://doi.org/10.1016/j.tecto.2017.10.004>
- van Horne, A., Sato, H., & Ishiyama, T. (2017). Evolution of the Sea of Japan back-arc and some unsolved issues. *Tectonophysics*, 710–711, 6–20. <https://doi.org/10.1016/j.tecto.2016.08.020>
- Vermeech, P. (2006a). Tectonic discrimination of basalts with classification trees. *Geochimica et Cosmochimica Acta*, 70(7), 1839–1848. <https://doi.org/10.1016/j.gca.2005.12.016>
- Vermeech, P. (2006b). Tectonic discrimination diagrams revisited. *Geochemistry, Geophysics, Geosystems*, 7(6), <https://doi.org/10.1029/2005GC001092>
- Wang, Z., Huang, R., Huang, J., & He, Z. (2008). P-wave velocity and gradient images beneath the Okinawa Trough. *Tectonophysics*, 455(1–4), 1–13. <https://doi.org/10.1016/j.tecto.2008.03.004>
- Warren, J. M. (2016). Global variations in abyssal peridotite compositions. *Lithos*, 248–251, 193–219. <https://doi.org/10.1016/j.lithos.2015.12.023>
- Wessel, P., & Müller, R. D. (2015). Plate tectonics. In G. Schubert Ed., *Treatise on geophysics* (2nd ed., pp. 45–93). Elsevier. chap. 6.0210.1002/2016JB012923. <https://doi.org/10.1016/B978-0-444-53802-4.00111-1>
- Whittaker, J. M., Müller, R. D., & Sdrolias, M. (2007). Revised history of Izanagi-Pacific ridge subduction. In *IBM07 NSF-margins workshop*.
- Wood, D. A. (1980). The application of a Th/HfTa diagram to problems of tectonomagmatic classification and to establishing the nature of crustal contamination of basaltic lavas of the British Tertiary Volcanic Province. *Earth and Planetary Science Letters*, 50(1), 11–30. [https://doi.org/10.1016/0012-821X\(80\)90116-8](https://doi.org/10.1016/0012-821X(80)90116-8)
- Woods, M. T., & Davies, G. F. (1982). Late Cretaceous genesis of the Kula plate. *Earth and Planetary Science Letters*, 58(2), 161–166. [https://doi.org/10.1016/0012-821X\(82\)90191-1](https://doi.org/10.1016/0012-821X(82)90191-1)
- Wright, N. M., Seton, M., Williams, S. E., & Müller, R. D. (2016). The Late Cretaceous to recent tectonic history of the Pacific Ocean basin. *Earth-Science Reviews*, 154, 138–173. <https://doi.org/10.1016/j.earscirev.2015.11.015>
- Wu, J., Suppe, J., Lu, R., & Kanda, R. (2016). Philippine Sea and East Asian plate tectonics since 52 Ma constrained by new subducted slab reconstruction methods. *Journal of Geophysical Research Solid Earth*, 121(6), 4670–4741. <https://doi.org/10.1002/2016JB012923>
- Wu, J. T.-J., & Wu, J. (2019). Izanagi-Pacific ridge subduction revealed by a 56 to 46 Ma magmatic gap along the northeast Asian margin. *Geology*, 47(10), 953–957. <https://doi.org/10.1130/G46778.1>
- Yamaji, A., & Yoshida, T. (1998). Multiple tectonic events in the Miocene Japan arc: The Heike microplate hypothesis. *Journal of Mineralogy Petroleum Economy Geology*, 93(10), 389–408. <https://doi.org/10.2465/ganko.93.389>
- Yamazaki, T., Takahashi, M., Iryu, Y., Sato, T., Oda, M., Takayanagi, H., et al. (2010). Philippine Sea Plate motion since the Eocene estimated from paleomagnetism of seafloor drill cores and gravity cores. *Earth Planets and Space*, 62(6), 495–502. <https://doi.org/10.5047/eps.2010.04.001>
- Zahirovic, S., Seton, M., & Müller, R. D. (2014). The cretaceous and cenozoic tectonic evolution of Southeast Asia. *Solid Earth*, 5(1), 227–273. 2014. <https://doi.org/10.5194/se-5-227-2014>
- Zhou, X. M., & Li, W. X. (2000). Origin of Late Mesozoic igneous rocks in Southeastern China: Implications for lithosphere subduction and underplating of mafic magmas. *Tectonophysics*, 326(3–4), 269–287. [https://doi.org/10.1016/S0040-1951\(00\)00120-7](https://doi.org/10.1016/S0040-1951(00)00120-7)
- Zijderveld, J. D. A. (1967). The natural remanent magnetizations of the Exeter volcanic traps (Permian, Europe). *Tectonophysics*, 4(2), 121–153. [https://doi.org/10.1016/0040-1951\(67\)90048-0](https://doi.org/10.1016/0040-1951(67)90048-0)